Final Technical Report (FTR)

| | |
|---|---|
| Project Title: | Higher Efficiency HVAC Motors |
| Award No.: | DE-EE0006721 |
| Award Type: | Cooperative Grant |
| Full Project Period: | 10/1/14 through 9/30/17 |
| Federal Agency: | Department of Energy |
| Sponsoring Office: | Energy Efficiency & Renewable Energy |
| FOA Name: | Building Energy Efficiency Frontiers and Incubator Technologies (BENEFIT) - 2014 |
| FOA Number: | DE-FOA-0001027 |
| Recipient: | QM Power, Inc. |
| | 9680 Marion Ridge |
| | Kansas City, MO 64137 |
| | www.qmpower.com |
| Recipient Type: | Private Company |
| Project Partners: | United Technologies Research Center (UTRC) |
| Principal Investigator (PI): | Charles Joseph (Joe) Flynn |
| | CEO & CTO |
| | 816-246-4200 |
| | jflynn@qmpower.com |
| DOE Project Team: | Contracting Officer: Geoffrey Walker |
| | Technology Manager: Antonio Bouza |
| | Project Officer: Jim Payne |
| | Project Engineer: Andrew Kobusch |
| | Grants Management Specialist: Mary Murray |

*Acknowledgment: "This material is based upon work supported by the U.S. Department of Energy's Office of Energy Efficiency and Renewable Energy (EERE) under the Award Number DE-EE0006721."*

**Executive Summary:**

The objective of this project was to design and build a cost competitive, more efficient heating, ventilation, and air conditioning (HVAC) motor than what is currently available on the market. Though different potential motor architectures among QMP's primary technology platforms were investigated and evaluated, including through the building of numerous prototypes, the project ultimately focused on scaling up QM Power, Inc.'s (QMP) Q-Sync permanent magnet synchronous motors from available sub-fractional horsepower (HP) sizes for commercial refrigeration fan applications to larger fractional horsepower sizes appropriate for HVAC applications, and to add multi-speed functionality. The more specific goal became the research, design, development, and testing of a prototype 1/2 HP Q-Sync motor that has at least two operating speeds and 87% peak efficiency compared to incumbent electronically commutated motors (EC or ECM, also known as brushless direct current (DC) motors), the heretofore highest efficiency HVACR fan motor solution, at approximately 82% peak efficiency. The resulting motor prototype built achieved these goals, hitting 90% efficiency and .95 power factor at full load and speed, and 80% efficiency and .7 power factor at half speed.

**Background:**

Q-Sync, developed in part through a DOE SBIR grant (Award # DE-SC0006311), is a novel, patented motor technology that improves on electronically commutated permanent magnet motors through an advanced electronic circuit technology. It allows a motor to "sync" with the alternating current (AC) power flow. It does so by eliminating the constant, wasteful power conversions from AC to DC and back to AC through the synthetic creation of a new AC wave on the primary circuit board (PCB) by a process called pulse width modulation (PWM; aka electronic commutation) that is incessantly required to sustain motor operation in an EC permanent magnet motor. The Q-Sync circuit improves the power factor of the motor by removing all failure prone capacitors from the power stage. Q-Sync's simpler electronics also result in higher efficiency because it eliminates the power required by the PCB to perform the obviated power conversions and PWM processes after line synchronous operating speed is reached in the first 5 seconds of operation, after which the PWM circuits drop out and a much less energy intensive "pass through" circuit takes over, allowing the grid-supplied AC power to sustain the motor's ongoing operation. Figure 1 illustrates the difference between Q-Sync and ECM by showing the voltage applied to the field coils of a Q-Sync motor compared to that within an ECM.

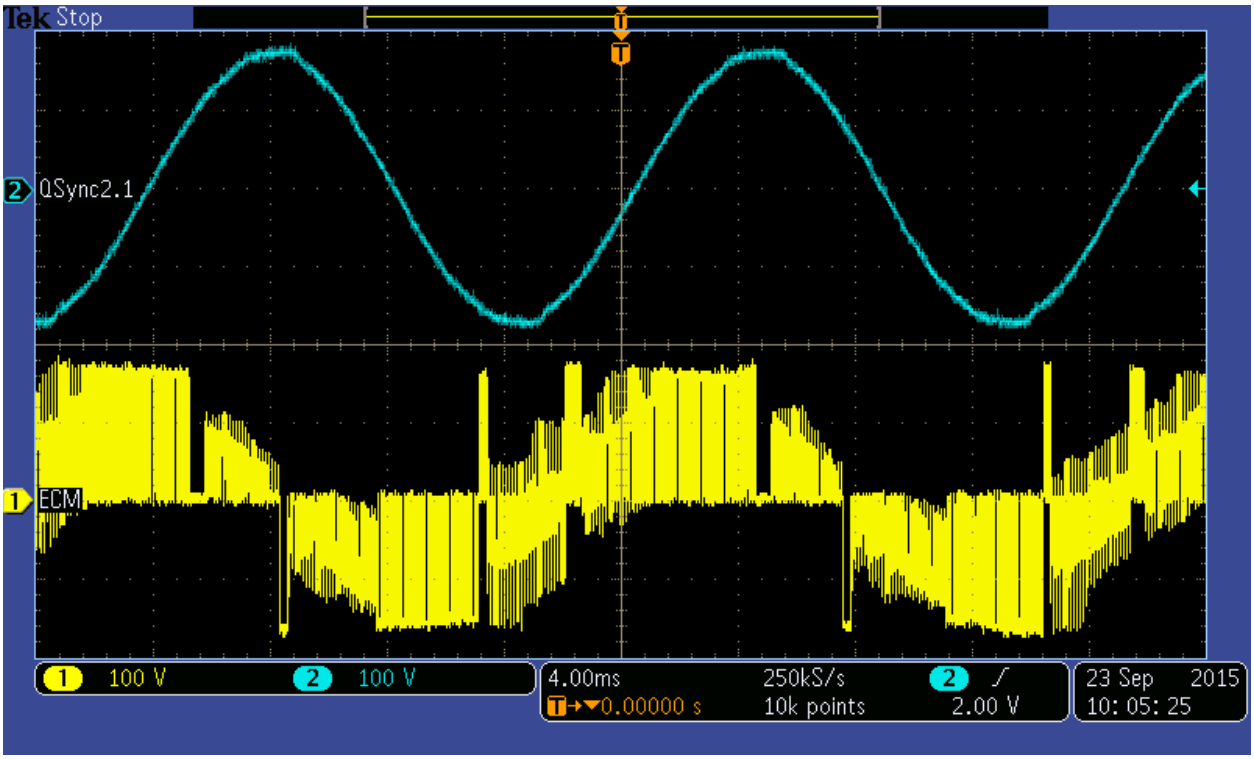


**Figure 1:** A sinusoidal wave courses through the field coils of a Q-Sync motor (on top) whereas a chopped synthetically created wave sustains the ECM; the black lines are indicative of losses

**Establishing the Target Application, Motor Specifications, & Performance Goals:**

In conjunction with project partner United Technologies Research Center (UTRC), it was determined that a nominal 1/2 HP (rated output), National Electrical Manufacturers Association (NEMA) 48 frame fan motor would be the target. These decisions were driven by both technical and market considerations and justifications were presented to the DOE project management team and agreed to before embarking on the design phases of the project. The much more complicated 20 HP compressor application that UTRC initially preferred was rejected as being overly complicated compared to the technological starting point, too expensive to build given the project budget, and lacking sufficient market volumes and savings potential to justify such an effort. Moreover, research led to the conclusion that the savings potential was greater upgrading fans compared to compressors.

One advantage of the 1/2 HP size is that they are utilized in both residential and smaller commercial HVAC applications, thus offering a high-volume target market. Moreover, 1/2 HP motors are used for condenser fans in commercial refrigeration, the market the initial Q-Sync motors are already addressing (for display case and walk-in unit evaporator fans with 1/60 HP and 1/15 HP motors, respectively), with expected quicker penetration via the refrigeration market reducing commercialization risks. Some of the key drivers of the decisions leading to the final choice are based on the report written by Navigant Consulting for the DOE's Buildings

Technologies Office entitled Energy Savings Potential and Opportunities for High-Efficiency Electric Motors in Residential and Commercial Equipment, published in December 2013[1]. Among other facts, the report posits that HVAC represents greater than 50% of technical energy savings potential in residential equipment, with fans representing well over 40% of that total, despite the fact that fan motors use less than 25% of total electricity in HVAC systems. The report estimates that fans can generate 2.8 times the energy savings as upgrading compressor motors could owing to the fact that most compressor motors already have close to 90% efficiencies whereas most installed fan motors are induction motors with efficiencies closer to 50-60%. In its examination of HVAC components, the report concludes that fans comprise 74% of technical energy savings potential compared to just 26% for compressors. The report also states central A/C outdoor fan upgrades have among the lowest payback periods at less than 1 year. The story is similar for the commercial market, with packaged terminal air conditioner (PTAC), single packaged vertical air conditioner (or heat pump) (SPVAC), and commercial unitary air conditioning (CUAC) HVAC products having an installed base of 17.3 million units and estimated 2012 shipments of 1.325 million units; the report holds that upgrading all small unitary fans would generate technical energy savings potential of .0507 quads, or 1.8 times the amount the next best compressor opportunity portends.

Once a fan application was settled on, QMP and UTRC worked together, with input from United Technology's Carrier unit, to settle on more detailed motor specifications for the R&D effort. A summary of the final specifications, target applications and performance goals can be found in Tables 1-3 immediately below.

| Metric Description | Metric Value |
|---|---|
| Application | Residential Furnace and Air Circulation Blower |
| Frame Size | NEMA 48 |
| Rating | 1/2 HP |
| Market Area | Worldwide |
| Major Competitors | Nidec, Regal Beloit |
| Warranty | 2 years |
| Target Envelope Size | 5.6" diameter x 10.2" long |
| Enclosure | Open Air |
| Bearings | Ball |
| Standard Shaft Connection | 0.5" diameter x 5.5" long, single flat 4.0" long |
| Standard Mounting Configurations | NEMA 48 with various adapters |
| Rotation | Reversible |
| Input Voltage | Selectable 115/208-230 VAC Single Phase 50/60 Hz |

[1] https://energy.gov/sites/prod/files/2014/02/f8/Motor%20Energy%20Savings%20Potential%20Report%202013-12-4.pdf

| | |
|---|---|
| Motor Speed | Variable 200-1200 rpm, 1075 rpm rated |
| Starting Torque | 1.9Nm |
| Full Load Efficiency | "up to 82%" (assume 80% at rated load) |
| Agency Certification | UL 1004-1, CSA, CE |
| Mechanical Reliability | <10% failure in 10 years |
| Environmental | Indoor/Outdoor |
| Operating Temperature Range | -40 to +55C |
| Control Interface | Programmable Speed and Direction |

| **Motor Application** |
|---|
| 1/2 HP Residential, Indoor/Outdoor Blower Motor |

| **Key Parameters and Goals** | | |
|---|---|---|
| **Description** | **Baseline** | **Goal** |
| Efficiency | 82% Peak | 87% |
| Cost - based upon single unit industrial supply house (Grainger) pricing for Regal Beloit Genteq part number 5SME39HXL110 Motor | $427.25 | Match |

**Tables 1-3:** Detailed Motor Specifications, Target Applications & Performance Goals

**Motor Design:**

In order to support our detailed design efforts, we tore down two competitive 1/3 HP products, one made by US Motors (then part of Emerson, now part of Nidec) and one by Genteq (Regal Beloit). Photos of the motors and internal components can be seen in Figures 2a-f and Figures 3a-f, respectively. Both motors are 3-phase, surface mounted permanent magnet rotor, electronically controlled synchronous motors. Both use low cost ferrite magnets and incorporate rather sophisticated approaches to low-cost manufacturing with some of the more unique features protected by patents. They each have encapsulated electronics for environmental protection so much of the circuitry is hidden, however, they appear to use fairly conventional rectifiers and 3-phase motor control modules.

The US Motors product is a 10 pole rotor, 12 stator slot configuration with concentrated coils. The rotor is made of 5 physical magnet segments each magnetized with two poles. The dividing line between the 2 poles is skewed, achieving the effect of traditional skewed laminations or magnets, reduced cogging torque, without the mechanical complications. The stator is unconventional in that the laminations are designed to be punched, stacked, and have coils

inserted on teeth as a linear assembly, which is then bent into a circle and welded. This arrangement sacrifices some flux path permeance but greatly simplifies winding and allows somewhat better copper fill.


**Figures 2a-f:** Internal components of a US Motors 1/3 HP blower motor

The Genteq motor, a 12 pole – 18 stator slot, takes a more conventional approach to rotor magnetization and stator assembly but utilizes a compliant rotor mount to mitigate vibration due to cogging.

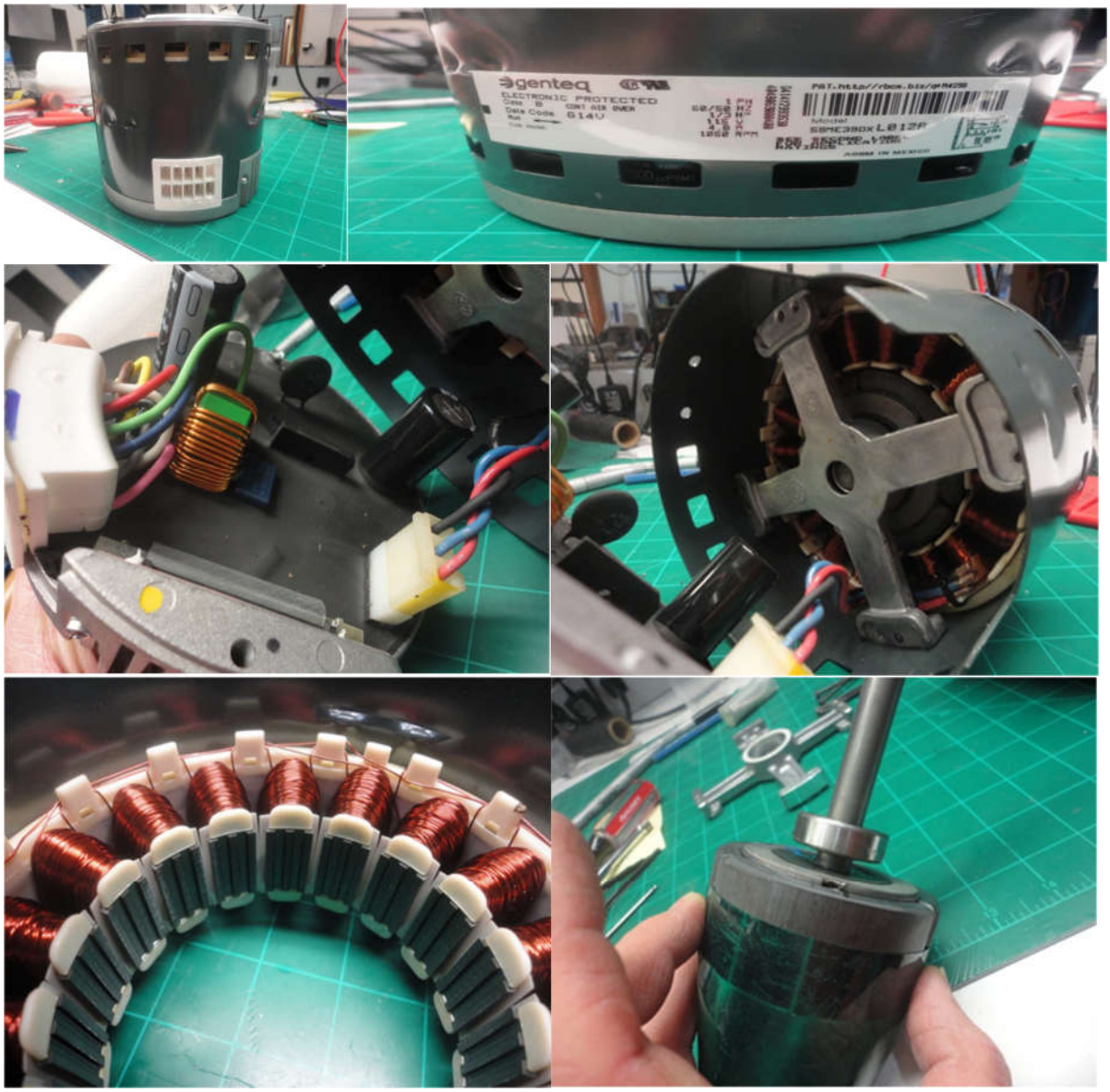


**Figures 3a-f:** Internal components of a Genteq 1/3 HP blower motor

In order to evaluate baseline performance, we also purchased an existing ½ HP blower motor (Genteq) from a local distributor and set it up our dynamometer to assess actual performance relative to our established project milestone specifications and goals. Figures 4 & 5 show the measured efficiency and power factor, respectively, versus speed with the motor set at each of the programmed torque set points ("taps") available on the control connector. Notice that the peak efficiency occurs at a minimum/lower load points and that the efficiency at the rating point, "hi tap" 1070 rpm is substantially lower. This is consistent with the "copper heavy" nature of the design as is indicated by the higher winding versus core losses calculated from the

preliminary analysis of the design. The best power factor occurs at the maximum load, as expected. The tests essentially confirm the assumed baseline peak efficiency levels in Table 3.

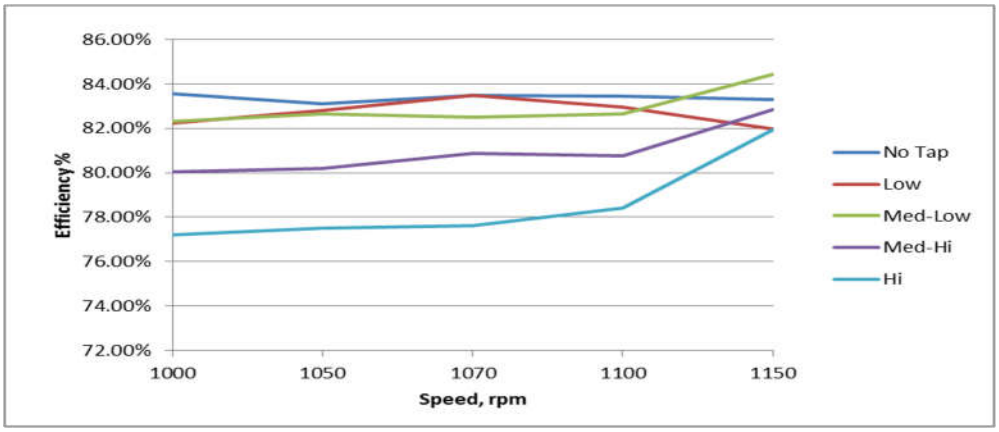


**Figure 4:** Efficiency curves on 1/2 HP Genteq Motor

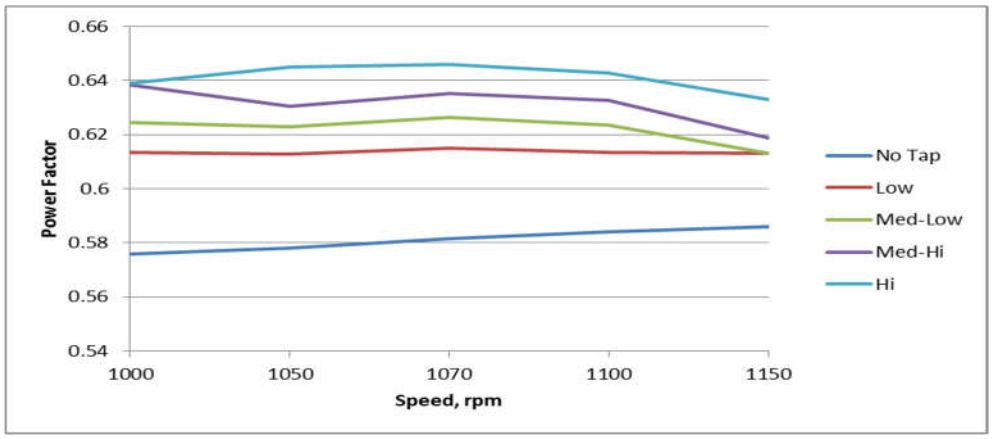


**Figure 5:** Power factor curves on 1/2 HP Genteq Motor

These efforts informed our preliminary analysis of possible motor configurations. Figure 6 below shows 4 permanent magnet motor configurations, from left to right: 1) a conventional surface mount magnet with an inside rotor; 2) a surface mount magnet outside rotor with QMP's isolated phase stator; 3) a QMP internal permanent magnet (IPM) rotor with an isolated phase stator; and 4) QMP's Q-Sync permanent magnet synchronous motor. Configuration 1 represents the majority of current products in the market. Configuration 2 generally provides higher torque density because of the larger air gap radius and, while it usually requires more expensive stator laminations due to higher frequency flux variation, it is used in cost sensitive electric bicycle applications and so was considered. Configuration 3 has been under development by QMP for larger motor and generator applications, with high efficiency and power density demonstrated. Configuration 4 represents QMP's currently available for sale low

power consuming fan products, which entail a favorable efficiency to cost ratio. Preliminary sizing analyses were performed on these configurations to assess their potential to meet the project goals.

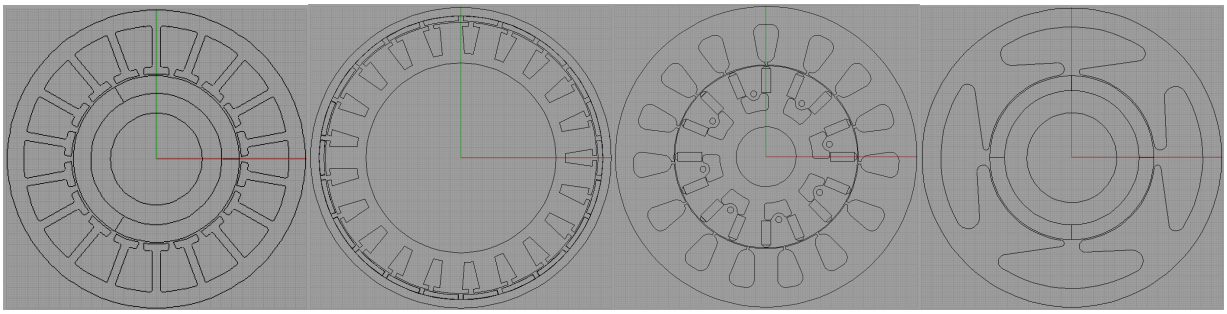

**Figure 6:** Incumbent & potential new motor configurations

The inquiry to determine which type of motor to focus work on was done by developing basic CAD models, performing magnetic finite element analyses, and making estimates of full load efficiencies and cost. Cost was estimated by applying a uniform cost model to all four designs using $/kg factors for magnetic components, evaluation of preliminary electronics designs, and rough estimates of relative cost mechanical components recognizing the relative complexity of any significant variations in the configurations. The cost factors are not intended to represent eventual production material costs, which are expected to be somewhat lower, but they do represent the relative costs of the designs for selection purposes. Table 4 shows a summary of the cost estimates and the efficiency calculations.

| | | Baseline Conventional ECM 12-pole | QM Power Internal PM ECM 10-pole | QM Power Outside Rotor ECM 22-pole | QM Power Q-Sync 4.0 6-Pole |
|---|---|---|---|---|---|
| **Material Cost** | **Total** | **$ 130.03** | **$ 133.90** | **$ 137.80** | **$ 128.71** |
| (estimated) | Stator core | $ 11.29 | $ 11.48 | $ 9.12 | $ 23.94 |
| | Winding | $ 20.38 | $ 20.28 | $ 18.28 | $ 30.12 |
| | Magnets | $ 7.85 | $ 7.13 | $ 3.38 | $ 8.01 |
| | Rotor core/hub | $ 9.00 | $ 13.50 | $ 25.50 | $ 9.00 |
| | Electroincs | $ 44.01 | $ 44.01 | $ 44.01 | $ 20.14 |
| | Mechanical | $ 30.00 | $ 30.00 | $ 30.00 | $ 30.00 |
| | Cords and connectors | $ 7.50 | $ 7.50 | $ 7.50 | $ 7.50 |
| **Power Loss** | **Efficiency** | **0.807** | **0.833** | **0.859** | **0.871** |
| | **Total, W** | **89.9** | **75.2** | **61.7** | **55.5** |
| | Core Loss | 8.87 | 13.82 | 10.02 | 5.85 |
| | Copper Loss | 52.39 | 32.75 | 23.05 | 28.19 |
| | Bearing & windage | 9.01 | 9.01 | 9.01 | 8.80 |
| | Electronics | 19.60 | 19.60 | 19.60 | 12.72 |

**Table 4:** Cost and efficiency estimates for the baseline and potential new motor configurations

The goal of this program is to achieve an efficiency improvement of at least 6% (87% versus an assumed baseline of 82%) without an increase in cost. The results indicate that the independent phase IPM design and the outside rotor design both have the potential for improved efficiency, but that they are likely to be higher cost solutions. The Q-Sync based design shows the most promise for meeting the program goal. In the case of the internal permanent magnet design, the somewhat increased complexity of the flux concentrating rotor results in moderate efficiency improvement due to better utilization of the copper, but expense increases. Further improvement in efficiency would require better, more expensive, core material or increased copper volume. The outside rotor design benefits from increased air gap diameter and a higher pole count to achieve nearly the desired efficiency. An increase in core losses normally associated with a higher pole count is avoided by the use of thinner laminations, which is possible because the stator, being on the inside, is of smaller diameter and uses much less material. However, while having the rotor on the outside is advantageous in certain applications, such as a directly attached external fan or for bicycle hub drives, it increases complexity and cost for the general purpose blower motor. The third possibility of scaling up QMP's Q-Sync technology represented a dramatically different approach since it is, at heart, an advanced electronic circuit technology rather than a novel motor architecture. This technology was originally developed as a low cost, high efficiency alternative to very low efficiency shaded pole and PSC induction motors and as a superior solution compared to relatively high cost ECM for fixed speed fan applications.

The Q-Sync design trades motor magnetic cost against electronics cost. This has proven effective in small, fixed speed fan motors that run in synchronism with line frequency; the thought was that there is an opportunity to run at high efficiency synchronous speeds at full speed (load) and use control mechanisms to allow for non-synchronous speeds, albeit at efficiencies more in line with ECM. The preliminary analysis, focused on the rated operating point, showed improved efficiency is indeed possible without increase in cost once the circuits and controls are fully developed. Continuing analysis was performed to further investigate the required wider operating range and control functionality required for the application, and would ultimately determine the viability of this configuration.

Figure 7 and Tables 5-7 on the following pages show design summary sheets resulting from magnetic FEA from these preliminary analyses. Related images of the QMP designs have been redacted due to their proprietary nature.

## Baseline Surface Magnet ECM (Genteq)

| | | | | | | | | |
|---|---|---|---|---|---|---|---|---|
| | Rated Power | 375 | W | | | | | |
| | Rated Speed | 1075 | rpm | Rated Torque | 3.33 | Nm | | |
| | BEMF | 124 | Vrms L-L | Elec Freq | 107.5 | Hz | | |
| | Poles | 12 | | Rated current | 1.746 | Arms | | |
| | Phases | 3 | | | | | | |
| | Rmeasured | 12.3 | Ohm L-L | X L-L | 57.41 | Ohm react | | |
| | L measured | 85 | mH L-L | | | | | |
| | | | | Copper loss | 52.39 | W | | |
| | Bearing/wind | 0.08 | Nm | Core loss | 8.87 | W | | |
| | Hotel power | 5 | W | Bearing loss | 9.01 | W | | |
| | Rectifier loss | 5.6 | W | electronic loss | 19.60 | W | | |
| | Drive bridge loss | 9 | W | Efficiency | 0.81 | | | |
| **Stator** | | | | | | | | |
| | Stack | 36.7 | mm | | | | | |
| | IR | 39.7 | mm | | | | | |
| | OR | 69.62 | mm | Stack vol | 188452 | mm^3 | | |
| | Number of slots | 18 | | Stack mass | 1.402 | kg | | |
| | lam area | 5134.5 | mm^2 | Tooth vol | 47951 | mm^3 | | |
| | tooth width | 3.81 | mm | Tooth mass | 0.357 | kg | Tooth B | 1.26 T |
| | Tooth length | 19.05 | mm | Tooth tip vol | 24856 | mm^3 | Tooth loss | 5.62 W |
| | Pole tip length | 3.25 | mm | Tooth tip mass | 0.185 | kg | Tooth tip B | 0.66 T |
| | Back iron thk | 7.62 | mm | Back vol | 115645 | mm^3 | Tip loss | 0.86 W |
| | Lam thickness | 0.8 | mm | Back mass | 0.860 | kg | Back B | 0.44 T |
| | Stacking factor | 0.95 | | Raw matl mass | 5.57 | kg | Back loss | 2.39 W |
| | Lam matl cost | 2.03 | $/kg | Stack cost | $ 11.29 | | Total Core loss | 8.87 W |
| **Winding** | | | | | | | | |
| | coils | 18 | | | | | | |
| | coil area | 137.9 | mm^2 | Cu Fill | 0.486 | | | |
| | coil form thk | 1 | mm | Avg turn length | 140.8 | mm | | |
| | coil mean radius | 52.5 | mm | Wire length/ph | 121674 | mm | | |
| | coil inside | 5.81 | mm | Cu vol/ph | 44456 | mm^3 | | |
| | coil outside | 18.32 | mm | Cu mass/ph | 0.396 | kg | | |
| | Turns | 144 | | Res/ph | 5.728 | Ohm | | |
| | Wire gauge | 21.5 | | Wire diameter | 0.682 | mm | | |
| | Wire cost | 15.00 | $/kg | Wire cost | $ 17.80 | | | |
| **Rotor** | | | | | | | | |
| | IR | 21.4 | mm | | | | | |
| | OR | 38.8 | mm | | | | | |
| | Stack | 46.0 | mm | | | | | |
| | Magnet thk | 8.1 | mm | Iron vol | 151289 | mm^3 | | |
| | Iron OR | 30.7 | mm | Iron mass | 1.150 | kg | | |
| | Magnets | 12 | | PM vol | 81308 | mm^3 | | |
| | Magnet grade | FB9 | | PM mass | 0.455 | kg | | |
| | PM matl cost | 17.25 | $/kg | PM cost | $ 7.85 | | | |

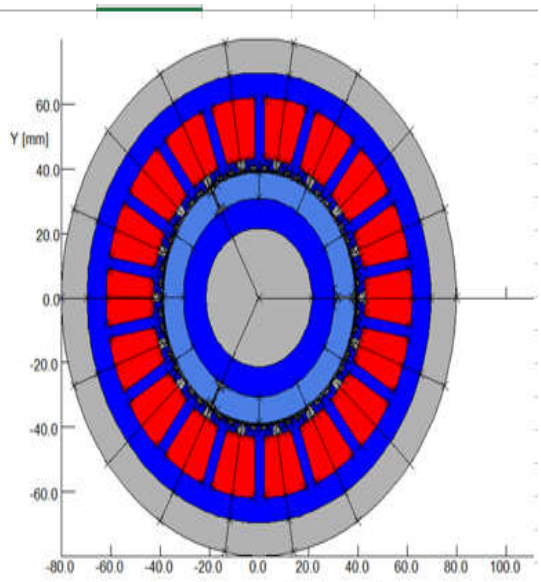


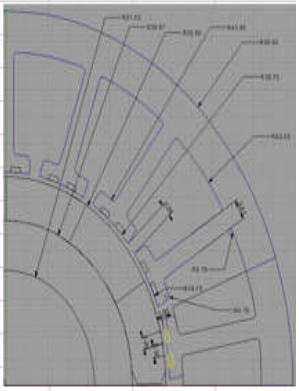

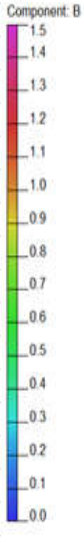


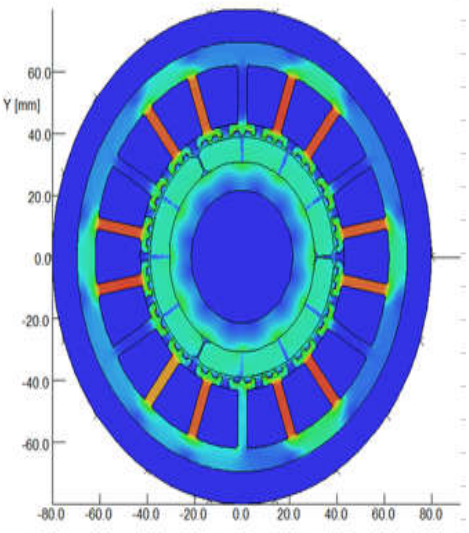


**Figure 7:** Baseline, 12-pole surface mounted magnet motor preliminary analysis

| | QM IPM | | | | | | | | |
|---|---|---|---|---|---|---|---|---|---|
| | Rated Power | 375 | W | | | | | | |
| | Rated Speed | 1075 | rpm | Rated Torque | 3.33 | Nm | | | |
| | BEMF | 124 | Vrms L-L | Rated current | 1.746 | Arms | | | |
| | Poles | 10 | | Elec Freq | 89.6 | Hz | | | |
| | Phases | 3 | | | | | | | |
| | Rmeasured | x | Ohm L-L | X L-L | x | Ohm react | | | |
| | L measured | x | mH L-L | | | | | | |
| | | | | Copper loss | 32.75 | W | | | |
| | Bearing/wind | 0.08 | Nm | Core loss | 13.82 | W | | | |
| | Hotel power | 5 | W | Bearing loss | 9.01 | W | | | |
| | Rectifier loss | 5.6 | W | electronic loss | 19.60 | W | | | |
| | Drive bridge loss | 9 | W | Efficiency | **0.83** | | | | |
| **Stator** | | | | | | | | | |
| | Stack | 38.0 | mm | | | | | | |
| | IR | 42 | mm | | | | | | |
| | OR | 69 | mm | Stack vol | 198018 | mm^3 | | | |
| | Number of slots | 9 | | Stack mass | 1.473 | kg | | | |
| | lam area | 5211 | mm^2 | Tooth vol | 48222 | mm^3 | | | |
| | tooth width | 9.4 | mm | Tooth mass | 0.359 | kg | Tooth B | 1.36 | T |
| | Tooth length | 15 | mm | Tooth tip vol | 40324 | mm^3 | Tooth loss | 4.71 | W |
| | Pole tip length | 5 | mm | Tooth tip mass | 0.300 | kg | Tooth tip B | 0.99 | T |
| | Back iron thk | 7 | mm | Back vol | 109472 | mm^3 | Tip loss | 2.18 | W |
| | Lam thickness | 0.8 | mm | Back mass | 0.815 | kg | Back B | 0.96 | T |
| | Stacking factor | 0.95 | | Raw matl mass | 5.67 | kg | Back loss | 6.92 | W |
| | Lam matl cost | 2.03 | $/kg | Stack cost | **$ 11.48** | | Total Core loss | **13.82** | W |
| **Winding** | | | | | | | | | |
| | coils | 9 | | | | | | | |
| | coil area | 198 | mm^2 | Cu Fill | 0.444 | | | | |
| | coil form thk | 1 | mm | Avg turn length | 213.2 | mm | | | |
| | coil mean radius | 54.5 | mm | Wire length/ph | 95924.7 | mm | | | |
| | coil inside | 11.4 | mm | Cu vol/ph | 44192 | mm^3 | | | |
| | coil outside | 38.05 | mm | Cu mass/ph | 0.393 | kg | | | |
| | Turns | 150 | | Res/ph | 3.581 | Ohm | | | |
| | Wire gauge | 20.5 | | Wire diameter | 0.766 | mm | | | |
| | Wire cost | 15.00 | $/kg | Wire cost | **$ 17.70** | | | | |
| **Rotor** | | | | | | | | | |
| | IR | 7 | mm | | | | | | |
| | OR | 41.33 | mm | | | | | | |
| | Lam area | 3339 | mm | | | | | | |
| | Stack | 46.0 | mm | | | | | | |
| | Magnet thk | 6.0 | mm | Iron vol | 1535940 | mm^3 | | | |
| | magnet width | 26.8 | mm | Iron mass | 11.673 | kg | | | |
| | Magnets | 10 | | PM vol | 73830 | mm^3 | | | |
| | Magnet grade | FB9 | | PM mass | 0.413 | kg | | | |
| | PM matl cost | 17.25 | $/kg | PM cost | **$ 7.13** | | | | |
| | | | | | | | | | |
| | | | | | | | | | |
| **Electroincs** | | | | | | | | | |
| | Output Module | 14.37 | $ 1kdigik | | | | | | |
| | Rectifier | | | | | | | | |
| | Filter Cap | | | | | | | | |

**Table 5:** QM Power Isolated Phase, IMP motor preliminary analysis

| QM Outside Rotor 22 pole Rev 2 | | | | | | | | | | |
|---|---|---|---|---|---|---|---|---|---|---|
| | Rated Power | 375 | W | | | | | | | |
| | Rated Speed | 1075 | rpm | Rated Torque | 3.33 | Nm | | | | |
| | BEMF | 124 | Vrms L-L | Rated current | 1.746 | Arms | | | | |
| | Poles | 22 | | Elec Freq | 197.1 | Hz | | | | |
| | Phases | 3 | | | | | | | | |
| | Rmeasured | x | Ohm L-L | X L-L | x | Ohm react | | | | |
| | L measured | x | mH L-L | | | | | | | |
| | | | | Copper loss | 23.05 | W | | | | |
| | Bearing/wind | 0.08 | Nm | Core loss | 10.02 | W | | | | |
| | Hotel power | 5 | W | Bearing loss | 9.01 | W | | | | |
| | Rectifier loss | 5.6 | W | electronic loss | 19.60 | W | | | | |
| | Drive bridge loss | 9 | W | Efficiency | **0.86** | | | | | |
| **Stator** | | | | | | | | | | |
| | Stack | 25.4 | mm | | | | | | | |
| | IR | 34 | mm | | | | | | | |
| | OR | 59.75 | mm | Stack vol | 89984.58 | mm^3 | | | | |
| | Number of slots | 21 | | Stack mass | 0.670 | kg | | | | |
| | lam area | 3542.7 | mm^2 | Tooth vol | 44592 | mm^3 | | | | |
| | tooth width | 4.4 | mm | Tooth mass | 0.332 | kg | Tooth B | 1.24 | T | |
| | Tooth length | 19 | mm | Tooth tip vol | 6307 | mm^3 | Tooth loss | 7.15 | W | |
| | Pole tip length | 2.5 | mm | Tooth tip mass | 0.047 | kg | Tooth tip B | 0.66 | T | |
| | Back iron thk | 4.25 | mm | Back vol | 39085.3 | mm^3 | Tip loss | 0.31 | W | |
| | Lam thickness | 0.5 | mm | Back mass | 0.291 | kg | Back B | 0.66 | T | |
| | Stacking factor | 0.95 | | Raw matl mass | 2.84 | kg | Back loss | 2.55 | W | |
| | Lam matl cost | 3.21 | $/kg | Stack cost | **$ 9.12** | | Total Core loss | **10.02** | W | |
| **Winding** | | | | | | | | | | |
| | coils | 21 | | | | | | | | |
| | coil area | 83.31 | mm^2 | Cu Fill | 0.854 | | | | | |
| | coil form thk | 1 | mm | Avg turn length | 100.3 | mm | | | | |
| | coil mean radius | 47.8 | mm | Wire length/ph | 75799.41 | mm | | | | |
| | coil inside | 6.4 | mm | Cu vol/ph | 39212 | mm^3 | | | | |
| | coil outside | 14.29 | mm | Cu mass/ph | 0.349 | kg | | | | |
| | Turns | 108 | | Res/ph | 2.520 | Ohm | | | | |
| | Wire gauge | 20 | | Wire diameter | 0.812 | mm | | | | |
| | Wire cost | 15.00 | $/kg | Wire cost | **$ 15.70** | | | | | |
| **Rotor** | | | | | | | | | | |
| | IR | 60.5 | mm | | | | | | | |
| | OR | 67 | mm | | | | | | | |
| | Stack | 25.4 | mm | | | | | | | |
| | Magnet thk | 2.5 | mm | | | | | | | |
| | magnet area | 62.7 | mm^2 | Iron vol | 41494.16 | mm^3 | | | | |
| | Iron IR | 63.0 | mm | Iron mass | 0.315 | kg | | | | |
| | Magnets | 22 | | PM vol | 35037 | mm^3 | | | | |
| | Magnet grade | FB9 | | PM mass | 0.196 | kg | | | | |
| | PM matl cost | 17.25 | $/kg | PM cost | **$ 3.38** | | | | | |
| | | | | | | | | | | |
| | | | | | | | | | | |
| **Electroincs** | | | | | | | | | | |
| | Output Module | 14.37 | $ 1kdigik | | | | | | | |
| | Rectifier | | | | | | | | | |
| | Filter Cap | | | | | | | | | |

**Table 6:** QM Power, 22-pole outside rotor preliminary analysis

| | Q-Sync 375W 6-pole | | | | | | | | |
|---|---|---|---|---|---|---|---|---|---|
| | Rated Power | 375 | W | | | | | | |
| | Rated Speed | 1050 | rpm | Rated Torque | 3.41 | Nm | | | |
| | BEMF | 100 | Vrms L-L | Rated current | 5.86 | Arms | | | |
| | Poles | 6 | | Elec Freq | 52.5 | Hz | | | |
| | Phases | 1 | | | | | | | |
| | Rmeasured | x | Ohm L-L | X L-L | x | Ohm react | | | |
| | L measured | x | mH L-L | PF at rated load | 0.8 | | | | |
| | | | | Copper loss | 28.19 | W | | | |
| | Bearing/wind | 0.08 | Nm | Core loss | 5.85 | W | | | |
| | Hotel power | 1 | W | Bearing loss | 8.80 | W | | | |
| | Rectifier loss | 0 | W | electronic loss | 12.72 | W | | | |
| | Drive bridge loss | 11.72 | W | Efficiency | **0.87** | | | | |
| **Stator** | | | | | | | | | |
| | Stack | 50.0 | mm | | | | | | |
| | IR | 34.75 | mm | | | | | | |
| | OR | 69 | mm | Stack vol | 300900 | mm^3 | | | |
| | Number of slots | 6 | | Stack mass | 2.239 | kg | | | |
| | lam area | 6018 | mm^2 | Tooth vol | 72000 | mm^3 | | | |
| | tooth width | 12 | mm | Tooth mass | 0.536 | kg | Tooth B | 1.32 | T |
| | Tooth length | 20 | mm | Tooth tip vol | 65537 | mm^3 | Tooth loss | 1.55 | W |
| | Pole tip length | 6.25 | mm | Tooth tip mass | 0.488 | kg | Tooth tip B | 0.75 | T |
| | Back iron thk | 8 | mm | Back vol | 163362.8 | mm^3 | Tip loss | 0.53 | W |
| | Lam thickness | 0.5 | mm | Back mass | 1.215 | kg | Back B | 1.05 | T |
| | Stacking factor | 0.95 | | Raw matl mass | 7.46 | kg | Back loss | 3.77 | W |
| | Lam matl cost | 3.21 | $/kg | Stack cost | $ **23.94** | | Total Core loss | **5.85** | W |
| **Winding** | | | | | | | | | |
| | coils | 6 | | | | | | | |
| | coil area | 351.7 | mm^2 | Cu Fill | 0.602 | | | | |
| | coil form thk | 1 | mm | Avg turn length | 206.7 | mm | | | |
| | coil mean radius | 51.0 | mm | Wire length/ph | 99231.32 | mm | | | |
| | coil inside | 14 | mm | Cu vol/ph | 206299 | mm^3 | | | |
| | coil outside | 32.04 | mm | Cu mass/ph | 1.836 | kg | | | |
| | Turns | 80 | | Res/ph | 0.821 | Ohm | | | |
| | Wire gauge | 14 | | Wire diameter | 1.627 | mm | | | |
| | Wire cost | 15.00 | $/kg | Wire cost | $ **27.54** | | | | |
| **Rotor** | | | | | | | | | |
| | IR | 18 | mm | | | | | | |
| | OR | 34 | mm | | | | | | |
| | Stack | 55.0 | mm | | | | | | |
| | Magnet thk | 8.0 | mm | Iron vol | 82938.05 | mm^3 | | | |
| | Iron OR | 26.0 | mm | Iron mass | 0.630 | kg | | | |
| | Magnets | 6 | | PM vol | 82938 | mm^3 | | | |
| | Magnet grade | FB9 | | PM mass | 0.464 | kg | | | |
| | PM matl cost | 17.25 | $/kg | PM cost | $ **8.01** | | | | |
| | | | | | | | | | |
| **Electroincs** | | | | | | | | | |
| | Output Module | $ 3.00 | 2 ea FET | | | | | | |
| | Rectifier | | | | | | | | |
| | Filter Cap | | | | | | | | |

**Table 7:** Q-Sync type 6-pole single phase motor preliminary analysis

Having identified the Q-Sync motor as most worthy of further investigation, some modifications were made to determine if coupling the Q-Sync circuit with other topologies would prove beneficial. More specifically, the Q-Sync based prototype motor design was updated to include an improved IPM PPMT rotor, thus incorporating motor architecture elements with the Q-Sync control mechanism. The improvement over previous designs come from eliminating the thin webs connecting the poles segments of the rotor lamination in order to reduce flux leakage while incorporating a rotor assembly method that does not result in the increased cost that would normally be associated with an increased part count and more elaborate assembly. Figure 8 shows a comparison between a traditional IPM rotor design and a design with no interconnecting webs (the mechanical assembly features are not shown). The elimination of the webs is particularly important for relatively low energy non-rare earth magnets, which are targeted to keep costs lower, from which up to 1/3 of the magnet flux can be lost to leakage.

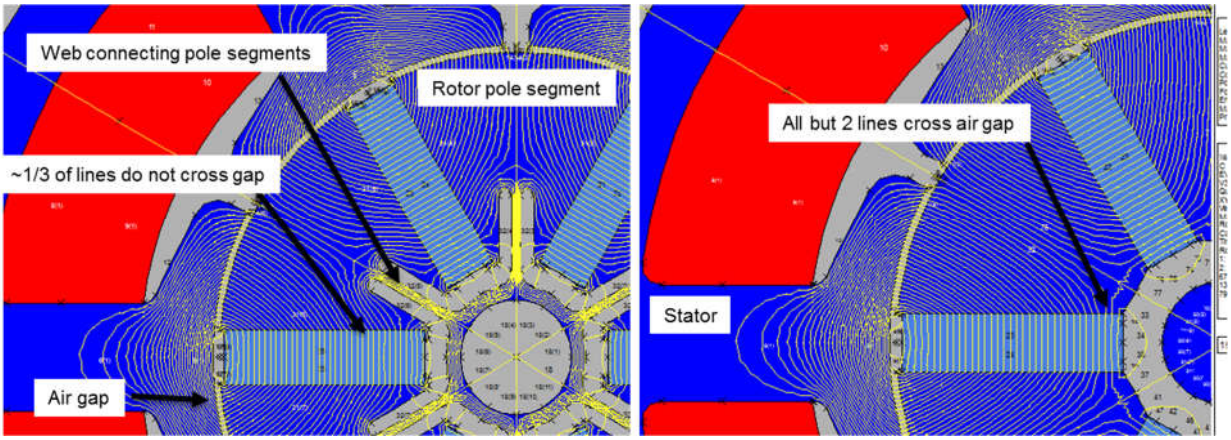


**Figure 8:** IPM rotor design; high leakage with connected segments (left), low leakage with separate segments (right)

Table 8 shows design summary sheets resulting from magnetic FEA (some of the images have been redacted due to their proprietary nature), and Table 9 shows the update comparison between the baseline design and the design configurations considered for this project. The estimated cost is based on material content but utilizes cost factors derived from current product production costs that include labor. For instance, the stator core cost is based on the known cost of a finished stator core multiplied by the ratio of the raw material content. Similarly, the winding cost is based on the cost of a finished winding. While there may be some differences in the details of assembly that are not captured by this approach, it still provided a reasonable basis for comparison because the designs are largely similar and similar assembly costs should be achievable through careful design for eventual manufacture.

| | Q-Sync 375W 6-pole | | | | | | | | |
|---|---|---|---|---|---|---|---|---|---|
| | Rated Power | 375 | W | | | | | | |
| | Rated Speed | 1050 | rpm | Rated Torque | 3.41 | Nm | | | |
| | BEMF | 110 | Vrms L-L | Rated current | 5.33 | Arms | | | |
| | Poles | 6 | | Elec Freq | 52.5 | Hz | | | |
| | Phases | 1 | | | | | | | |
| | Rmeasured | x | Ohm L-L | X L-L | x | Ohm react | | | |
| | L measured | x | mH L-L | PF at rated load | 0.8 | | | | |
| | | | | Copper loss | 23.29 | W | | | |
| | Bearing/wind | 0.08 | Nm | Core loss | 7.01 | W | | | |
| | Hotel power | 1 | W | Bearing loss | 8.80 | W | | | |
| | Rectifier loss | 0 | W | electronic loss | 11.65 | W | | | |
| | Drive bridge loss | 10.65 | W | Efficiency | **0.88** | | | | |
| **Stator** | | | | | | | | | |
| | Stack | 50.0 | mm | | | | | | |
| | IR | 34.75 | mm | | | | | | |
| | OR | 69 | mm | Stack vol | 300900 | mm^3 | | | |
| | Number of slots | 6 | | Stack mass | 2.239 | kg | | | |
| | lam area | 6018 | mm^2 | Tooth vol | 72000 | mm^3 | | | |
| | tooth width | 12 | mm | Tooth mass | 0.536 | kg | Tooth B | 1.32 | T |
| | Tooth length | 20 | mm | Tooth tip vol | 65537 | mm^3 | Tooth loss | 1.86 | W |
| | Pole tip length | 6.25 | mm | Tooth tip mass | 0.488 | kg | Tooth tip B | 0.75 | T |
| | Back iron thk | 8 | mm | Back vol | 163362.8 | mm^3 | Tip loss | 0.63 | W |
| | Lam thickness | 0.5 | mm | Back mass | 1.215 | kg | Back B | 1.05 | T |
| | Stacking factor | 0.95 | | Raw matl mass | 7.46 | kg | Back loss | 4.52 | W |
| | Lam matl cost | 2% | %/kg | Stack cost | **18%** | | Total Core loss | **7.01** | W |
| **Winding** | | | | | | | | | |
| | coils | 6 | | | | | | | |
| | coil area | 351.7 | mm^2 | Cu Fill | 0.602 | | | | |
| | coil form thk | 1 | mm | Avg turn length | 206.7 | mm | | | |
| | coil mean radius | 51.0 | mm | Wire length/ph | 99231.32 | mm | | | |
| | coil inside | 14 | mm | Cu vol/ph | 206299 | mm^3 | | | |
| | coil outside | 32.04 | mm | Cu mass/ph | 1.836 | kg | | | |
| | Turns | 80 | | Res/ph | 0.821 | Ohm | | | |
| | Wire gauge | 14 | | Wire diameter | 1.627 | mm | | | |
| | Wire cost | 12% | %/kg | Wire cost | **21%** | | | | |
| **Rotor** | | | | | | | | | |
| | IR | 18 | mm | | | | | | |
| | OR | 34 | mm | | | | | | |
| | Stack | 55.0 | mm | | | | | | |
| | Magnet thk | 8.0 | mm | Iron vol | 82938.05 | mm^3 | | | |
| | Iron OR | 26.0 | mm | Iron mass | 0.630 | kg | | | |
| | Magnets | 6 | | PM vol | 60720 | mm^3 | | | |
| | Magnet grade | FB9 | | PM mass | 0.340 | kg | | | |
| | PM matl cost | 13% | %/kg | PM cost | 5% | | | | |
| | | | | | | | | | |
| **Electroincs** | | | | | | | | | |
| | Output Module | $ 3.00 | 2 ea FET | | | | | | |
| | Rectifier | | | | | | | | |
| | Filter Cap | | | | | | | | |

**Table 8:** Q-Sync based motor with IPM PPMT rotor preliminary design

| | | Conventional ECM 12-pole | IPM PPMT ECM 10-pole | Outside Rotor ECM 22-pole | IPM PPMT Q-Sync 4.0 6-Pole |
|---|---|---|---|---|---|
| **Material Cost** | **Total** | **100.0%** | **103.0%** | **106.0%** | **100.0%** |
| (estimated) | Stator core | 8.7% | 8.8% | 7.0% | 18.4% |
| | Winding | 15.7% | 15.6% | 14.1% | 23.2% |
| | Magnets | 6.0% | 5.5% | 2.6% | 4.5% |
| | Rotor core/hub | 6.9% | 10.4% | 19.6% | 8.8% |
| | Electroincs | 33.8% | 33.8% | 33.8% | 17.0% |
| | Mechanical | 23.1% | 23.1% | 23.1% | 22.4% |
| | Cords and connectors | 5.8% | 5.8% | 5.8% | 5.8% |
| **Power Loss** | **Efficiency** | **0.800** | **0.826** | **0.852** | **0.879** |
| | **Total, W** | **93.6** | **79.1** | **65.0** | **51.8** |
| | Core Loss | 10.77 | 15.94 | 11.56 | 7.01 |
| | Copper Loss | 52.39 | 32.75 | 23.05 | 23.29 |
| | Bearing & windage | 8.80 | 8.80 | 8.80 | 8.80 |
| | Electronics | 21.60 | 21.60 | 21.60 | 12.72 |

**Table 9:** Updated cost and efficiency results for the IPM PPMT Q-Sync alternate design

In order to further refine the electromechanical design and develop the drive electronics and control strategy, a detailed FEA model was created with coupled drive circuits. Figure 9 shows the model and typical flux plot.

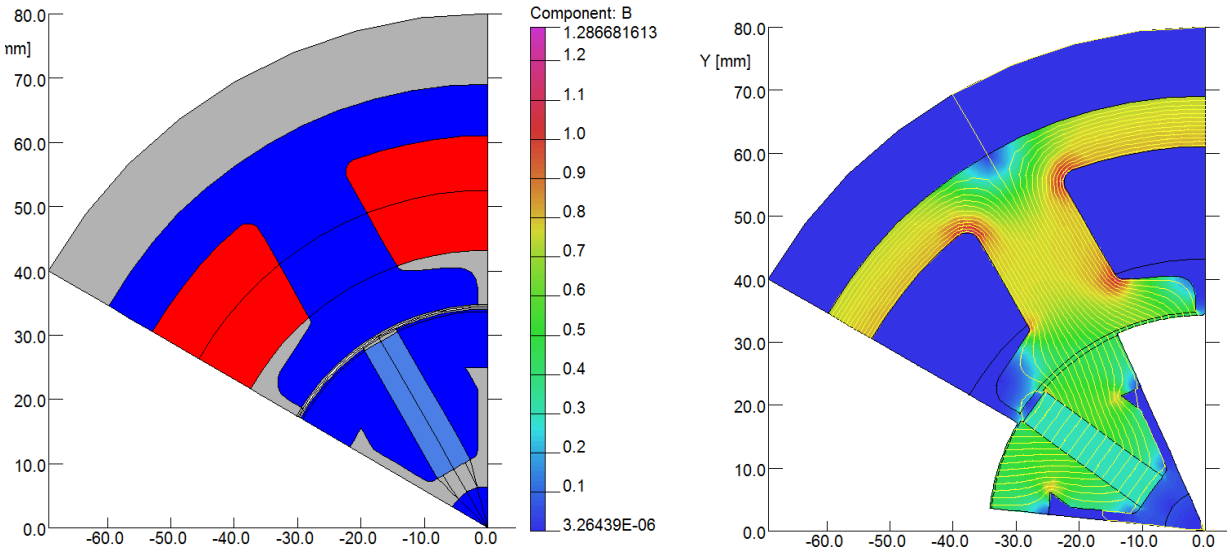


**Figure 9:** Detailed magnetic FEA was performed with the coupled drive circuit to verify performance predictions

With the prototype configurations chosen and the electromagnetic modeling complete, a detailed mechanical design was generated. A key element is the IPM rotor assembly, shown conceptually in Figure 10, which will utilize automated placement of laminations, magnets and shaft into a mold. Semitransparent and partially exploded isometric views of the complete mechanical model for the IPM Q-Sync prototypes, and top assembly drawings were prepared, but they are not included in this report due to their proprietary nature.

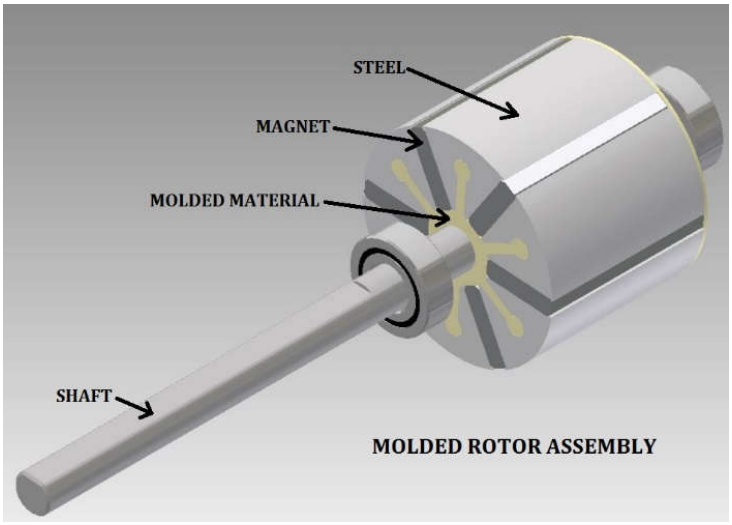


**Figure 10:** Concept for cost effective IPM rotor construction with molded hub and separate pole segments for low flux leakage

The initial prototype design having been determined, initial drive design work began, focusing on a single phase ECM controller, which was used to estimate cost of the more conventional motor design options. Our selection of a Q-Sync based prototype motor design relies on the fact that the Q-Sync approach requires fewer components, greatly reducing the cost of the drive. The key to higher efficiency and power factor is running the motor synchronously off the line voltage without power conversion. The control circuit is only active during starting (and during abnormal load transients), thus eliminating power conversion losses during normal operation. The HVAC application requires variable speed/torque operation and so this concept cannot be directly applied. However, an adaptation of the circuit has been developed for 12W to preserve the benefit of minimal power conversion and allow for variable speed operation. Figure 11 shows the 12W demonstration unit on the engineering test bench. Testing has shown that much of the power factor benefit is preserved for operation over certain speed ranges.

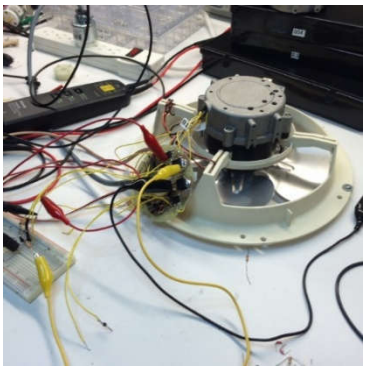

**Figure 11:** 12W Q-Sync product modified for variable speed operation

The application of this concept for the project required a significant scaling up of power levels. In order to investigate the issues associated with the scaling up we created a "quick and dirty" ½ HP demonstration by modifying a single phase ½ HP induction motor. The squirrel cage rotor was removed and replaced with a simple permanent magnet rotor made with off-the-shelf components. A breadboard Q-Sync circuit was constructed with larger power rating components. Figure 12 shows the motor fitted with a fan for testing. The motor is mounted on, but for this demonstration not connected to, our 1 HP 4-quadrant dynamometer seen in the left edge of the photograph. Dyno testing to date indicates that the expected high efficiency and power factor are achieved for fixed speed Q-Sync operation. Work then focused on adapting the variable speed controls of the 12 watt motor to control the current in the larger motor with its much lower impedance.

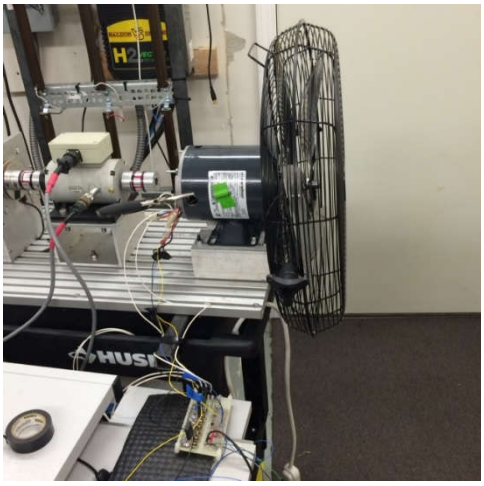

**Figure 12:** ½ HP motor modified for demonstration with Q-Sync controls

With analysis having shown that the program goals documented would be theoretically achievable with the contemplated design, the project manager gave the go-ahead to begin

fabrication of a prototype. Figure 13 summarizes the results justifying the prototype building decision.

**Goal: 87% Efficiency at Same Cost**

- Performance analysis result giving 88% efficiency at full load.
- Cost analysis showing less or equal to baseline
- Best engineering estimates based on experience and initial supplier feedback are consistent with $427.25 single unit retail at industrial supply house.

| | | Efficiency | 88% |
|---|---|---|---|
| **Rated Output** | | **W** | **375** |
| **Power Loss** | | **Total, W** | **50.8** |
| | Core Loss | | 7.01 |
| | Copper Loss | | 23.29 |
| | Bearing & windı | | 8.80 |
| | Electronics | | 11.65 |

| Cost Components | | Total | $ | 88.26 |
|---|---|---|---|---|
| (estimated) | Stator core | | $ | 15.96 |
| | Insulation and Varnish | | $ | 2.58 |
| | Winding | | $ | 3.00 |
| | Wire | | $ | 11.02 |
| | Magnets | | $ | 3.06 |
| | Rotor core/hub | | $ | 3.00 |
| | Shaft and bearings | | $ | 2.00 |
| | Rotor assembly | | $ | 1.50 |
| | Electroincs | | $ | 20.14 |
| | Case and flanges | | $ | 18.00 |
| | hardware | | $ | 2.00 |
| | Cords and connectors | | $ | 6.00 |

**Figure 13:** Summary of prototype design analysis results versus project goals

We thus began fabrication of the initial motor and drive prototypes. One of the major efforts was the construction of an IPM rotor using individual pole segments and magnets bonded to the shaft with a molded hub, as illustrated above in Figure 10. In order to accelerate initial motor testing, debugging of electronics, and control software optimization, the development of an alternate rotor was designed using more readily available (off-the-shelf) rare earth Neodymium-Iron-Boron (NdFeB) magnets. The NdFeB magnets are much stronger and so the rotor lamination was designed for much smaller magnets to achieve equivalent air gap flux and performance. Figure 14 shows a side-by-side comparison of predicted flux density for the ferrite and NdFeB designs indicating that the NdFeB versions have slightly higher flux density values. They matched close enough for debugging the system and evaluation of the fundamental design. We also assembled and began winding the stator. A breadboard prototype of the motor drive was also fabricated. For convenience of initial evaluation and controls development, this prototype used a full featured processor development board in place of the embedded processor of the final design, which was wired to a custom circuit board with the rest of the power and signal components.

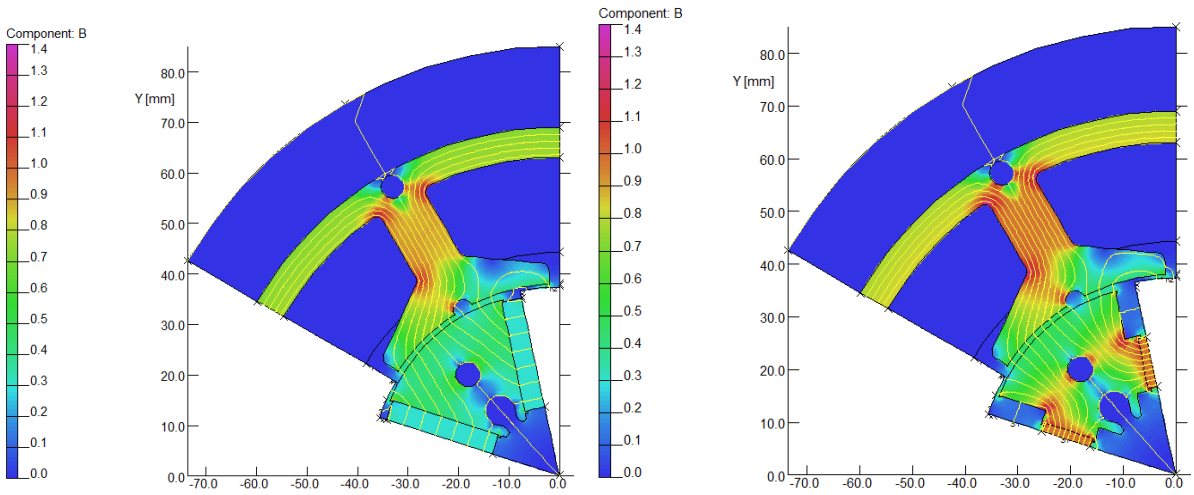


**Figure 14:** Analysis of the prototype rotor design using ferrite magnets, left, and an initial test motor using much smaller but much stronger NdFeB magnets, right

The prototype process for building the rotor can be labor intensive; however, the tooling required for the said process is simple and was perfected by our team. The steps are:

- Laser cutting the individual rotor segment lamination from a 0.5 mm sheet (see Figure 15)
- Stacking to make full length (55mm) rotor pole segments
- Assembling the pole segments, magnets and motor shaft into position on a fixture
- Pouring a 2-part urethane material into the hub cavity
- Oven curing the urethane

Figures 16 & 17 show images of the completed initial prototypes with the NdFeB rotor. For production, the lamination segments would be punched versus laser cut, automated tooling utilized to directly stack the lamination and insert the magnets. The use of a thermoplastic material to replace the urethane (a thermoset material), eliminating the need for oven curing, will be considered.

**Figure 15:** Laser cut individual rotor pole lamination for the NdFeB design


**Figure 16:** Rotor pole pieces assembled on a fixture with the magnets in preparation for casting the urethane hub; the motor shaft would also be inserted in the fixture prior to casting

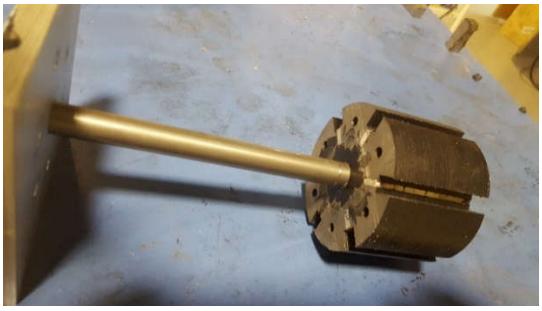

**Figure 17:** Prototype rotor assembly after curing of the urethane and removal from the fixture

The prototype stator fabrication followed a process similar to what we had used for other motor products. The major components are the stator stack made up of individual laminations cut from a 0.5mm thick sheet on our laser cutter (see Figure 18), plastic coil forms that keep the coil ends in place, and the wound coils. The production coil forms would be injection molded parts. For the prototype, coil forms were made using a urethane casting in a simple silicon mold. The silicon mold was made using a 3-D printed sample part as a plug for casting the silicon rubber. The coils for the prototype were hand wound into place. Figure 19 shows the partially wound prototype stator, which was subsequently finished.

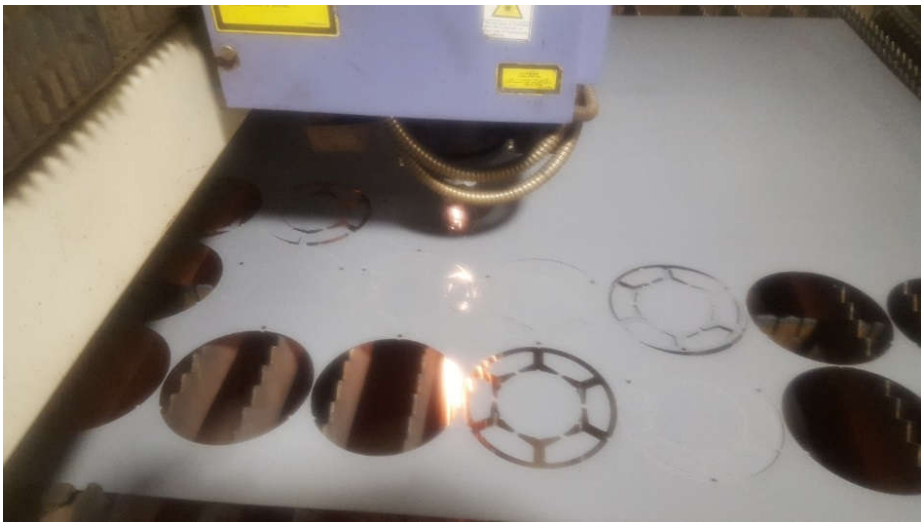

**Figure 18:** Stator laminations being laser cut in the QM Power shop

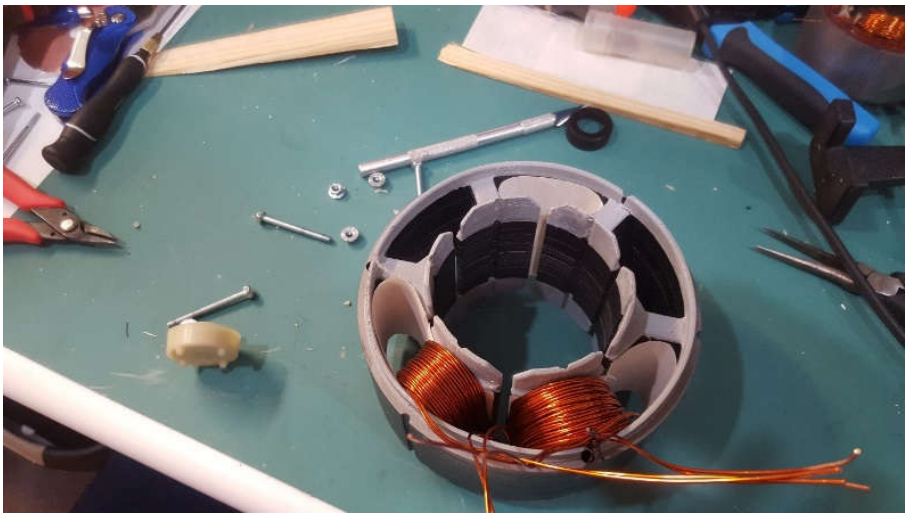

**Figure 19:** Hand winding of the first prototype stator in process

A breadboard circuit of the prototype design was fabricated for initial circuit controls debugging and evaluation. This breadboard consisted of two separate circuit cards: a power and signal card with actual prototype design circuits, and an off-the-shelf processor evaluation board. These boards are shown in Figures 20 and 21. This configuration was chosen to facilitate software and controls development. Once we demonstrated function of the drive the plan was to lay out a single board with all circuits and the processor with the mechanical shape and connection and mounting features to fit the actual prototype motor.

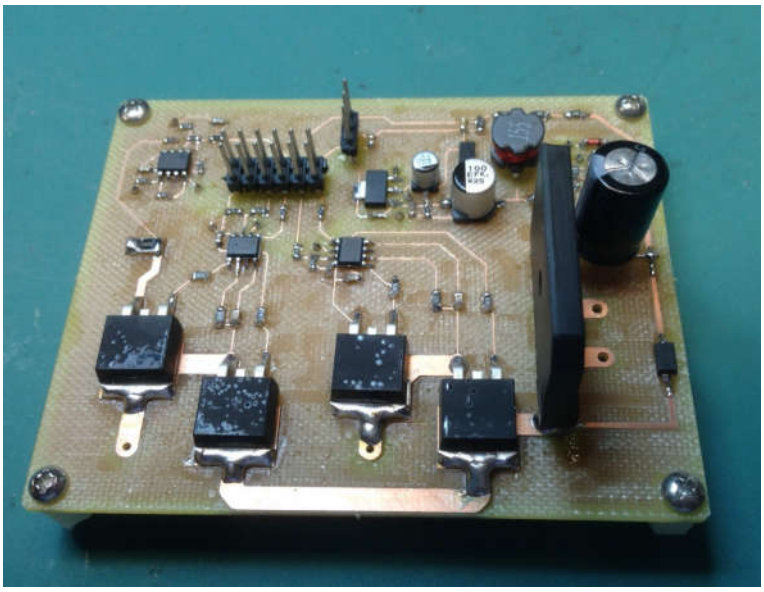

**Figure 20:** Breadboard prototype drive electronics for evaluation with external microprocessor

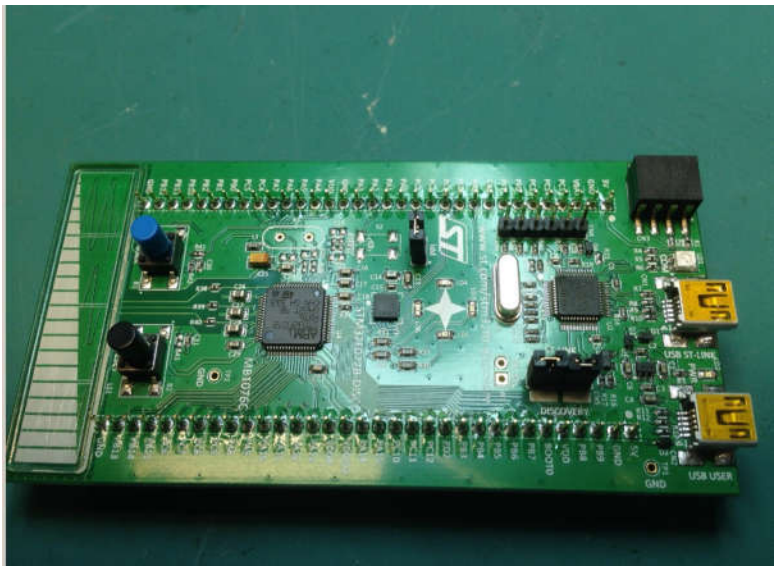

**Figure 21:** Microprocessor development board to be used with breadboard electronics

We completed fabrication of the first breadboard prototype with simplified mechanical components (end housings) and, for initial testing, a rotor using off the shelf Neo magnets for rapid assembly to accelerate drive development. Figure 22 is an image of the first prototype. Having received the custom made lower cost, production intent, ferrite magnets, another rotor

assembly was made (see Figure 23). This second rotor would eventually be substituted into the assembly for evaluation.

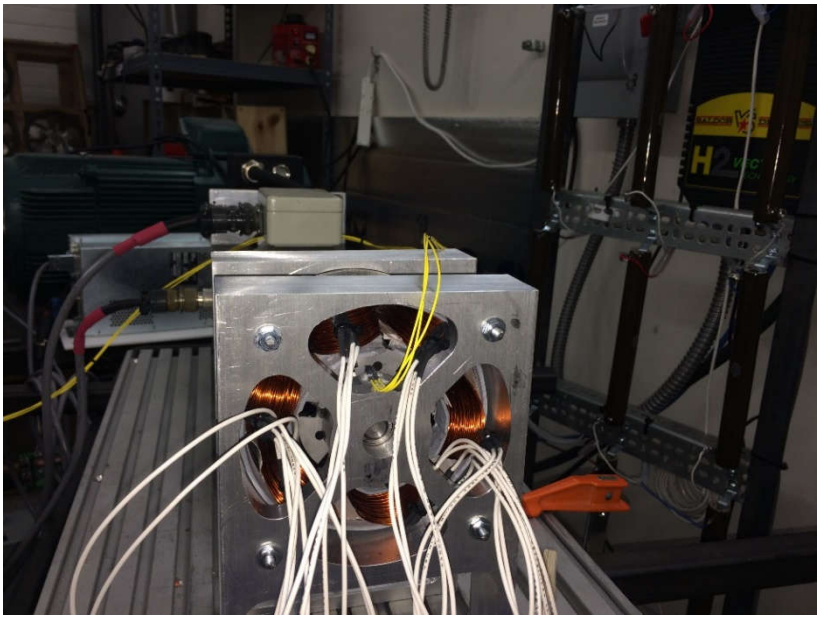

**Figure 22:** The "breadboard" first prototype motor set up for testing and drive development

**Figure 23:** The second IPM rotor with production intent ferrite magnets

At this time, some additional manufacturing refinements were also added to the full mechanical prototype design and a full 3D printed mockup was generated to better visualize the assembly. Figure 24 shows the revised full assembly drawing.

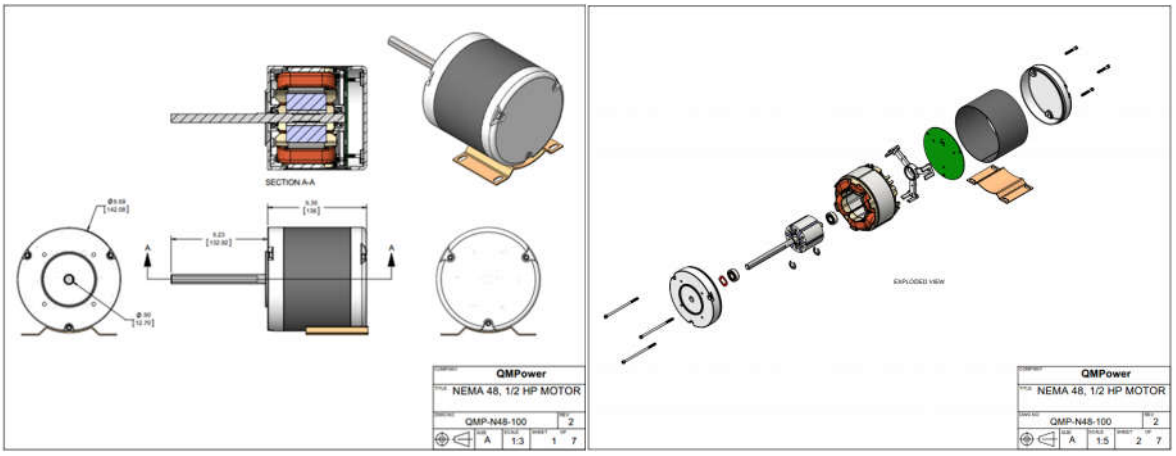


**Figure 24:** Revised full prototype mechanical design

The second prototype rotor and a second stator assembly were fabricated along with a complete set of mechanical housing components in order to assemble our first full mechanical prototype, shown in Figure 25.


**Figure 25:** First complete mechanical prototype

Controls debugging and circuit refinement began with the breadboard drive. Figure 26 shows the initial set up for evaluating functionality with our 12W motor. A final form factor printed writing board (PWB) layout was generated, with fabrication pending final input from the breadboard evaluation.

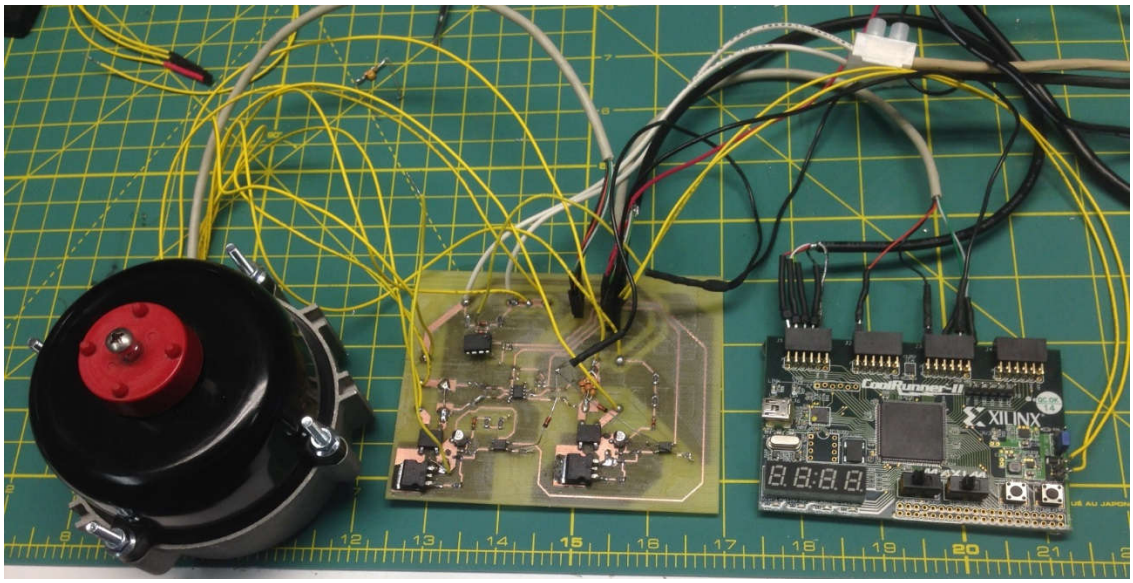


Figure 26: Breadboard prototype drive electronics undergoing initial evaluation with our existing 12W motor

We began controller tuning and testing with the breadboard electronics and the first prototype motor assembly (see Figure 27) in advance of bringing this configuration up to full power, finalizing the drive circuit and fabricating the full prototype control board, and integrating it with the full mechanical prototype motor.

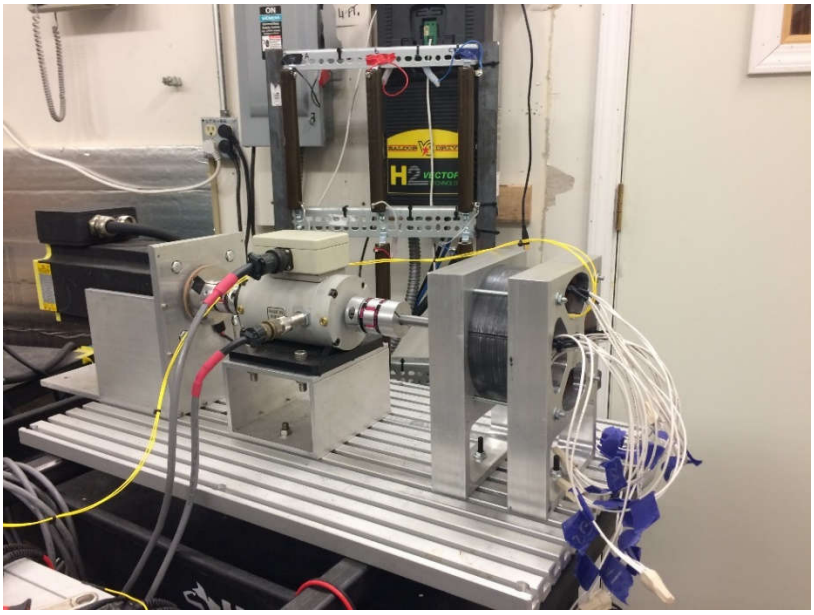

**Figure 27:** Breadboard prototype drive electronics and motor set up on our 4-quadrant dynamometer for preliminary drive tuning and testing

Initial testing of the first full mechanical prototype suggested additional changes were required. Testing has revealed excessive mechanical vibration and associated acoustic noise. The source was traced to torsional and axial vibrations of the rotor due to low stiffness of the bearing mounts. The mechanical design was modified by adding stiffening ribs to the front cover and increasing the thickness of the arms of the rear bearing support.

We then fabricated a second prototype, shown in Figure 28, which demonstrated greatly reduced mechanical vibration and noise. Final noise assessment would be made using motor mounting more representative of the final application once controller development and tuning are complete.

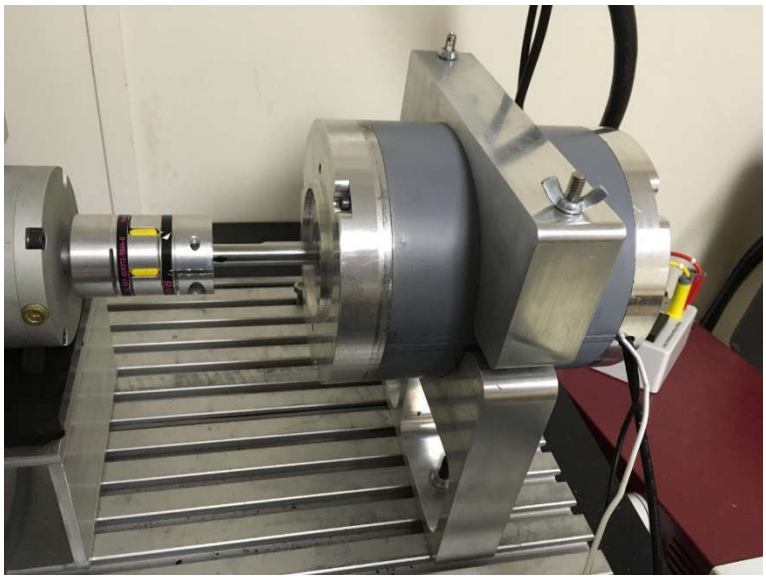

**Figure 28:** Full prototype assembly with improved mechanical design for reduced vibration

Regarding controller development and tuning, we concluded that our motor drive approaches were not meeting project goals for efficiency and power output. The first approach, a modified H-bridge, fell 1-2% short of target efficiency, and the second, Q-Sync generation 4.2, must be de-tuned to control inductive voltage spikes to the point where it no longer produced sufficient torque. We therefore began working on a new variation of the Q-Sync technology more properly considered multi-speed versus variable speed. Conceptually, this approach avoids the inductive voltage and/or losses associated with hard current turn off by operating a fixed number of speeds rather than allowing continuously variable speed.

Final form factor printed circuit assemblies were fabricated for two implementations of our initial modified H-Bridge motor drive, one using an integrated power module and one using lower conduction loss discrete MOSFETs. Both were integrated with the prototype stator and

preliminary assessment of performance was made using various switching patterns. The MOSFET version showed generally better performance, however peak efficiency was 1-2% short of the project goal of 87%. Figure 29 shows images of the drive assemblies.

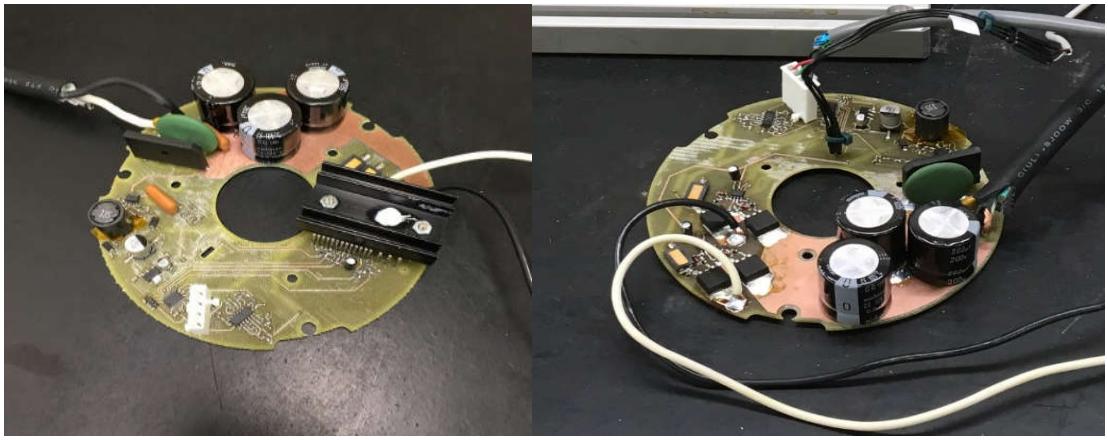

**Figure 29:** Prototype motor drive assemblies, integrated power module and discrete MOSFET versions

A second motor drive approach based on our Q-Sync generation 4.2 technology was evaluated by fabricating a breadboard motor drive, shown in Figure 30, and testing it with the prototype stator. Our in-production fixed, synchronous speed fan motors use a single phase set of stator coils and produce very large, and low frequency, torque harmonics when operating at off-synchronous speeds. The generation 4.2 Q-Sync uses two sets of coils with opposite polarities to greatly reduce torque ripple at off-synchronous operation. The generation 4.2 also better times when coils are switched off to reduce energy loss and high voltage spikes due to energy stored in the coil inductance. However, after extensive tuning of the switching pattern using the breadboard system, we were not able to sufficiently reduce that energy loss without significantly reducing the average torque due to reduction in the effective duty cycle.

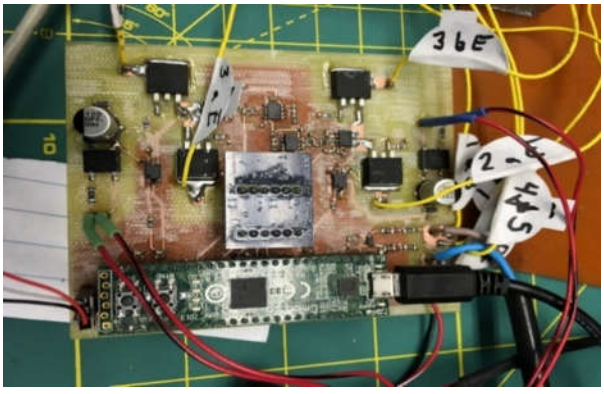


**Figure 30:** Breadboard Q-Sync Generation 4.2 controller

In light of the limitations encountered in our first two controller configurations, we decided to pursue a new variation of the Q-Sync technology being developed for 2-speed fan applications that require efficient operation at two fixed speeds: line synchronous speed and at exactly one-half line synchronous speed. This is achieved by having twice the number of stator teeth as rotor poles and arranging the stator coils and switching network such that the stator poles will step one revolution per AC cycle or ½ revolution per AC cycle. This concept can be extended by using other combinations of stator teeth and rotor poles to create a motor with a number of efficient, fixed speed operating points. We are calling this a multi-speed drive as opposed to a variable speed drive. An initial two speed demonstration utilized our existing 50W fan motor product. Modeling and simulation was undertaken for extension to a ½ HP multi-speed solution for the HVAC blower application, planned for after proving the concept in the 50W motor with a breadboard control circuit.

The 4.2 circuit was then modified by adding a third MOSFET to provide a path for transfer of the inductive energy between the two sets of coils when one set is turned off. The breadboard assembly of this circuit is shown in Figure 31. Initial tuning of the circuit was performed using the prototype ½ HP motor installed in a condenser fan assembly, as shown in Figure 32. Preliminary qualitative results showed good control and greatly improved torque capability, the major deficiency of the previous 4.2 Q-Sync circuit.

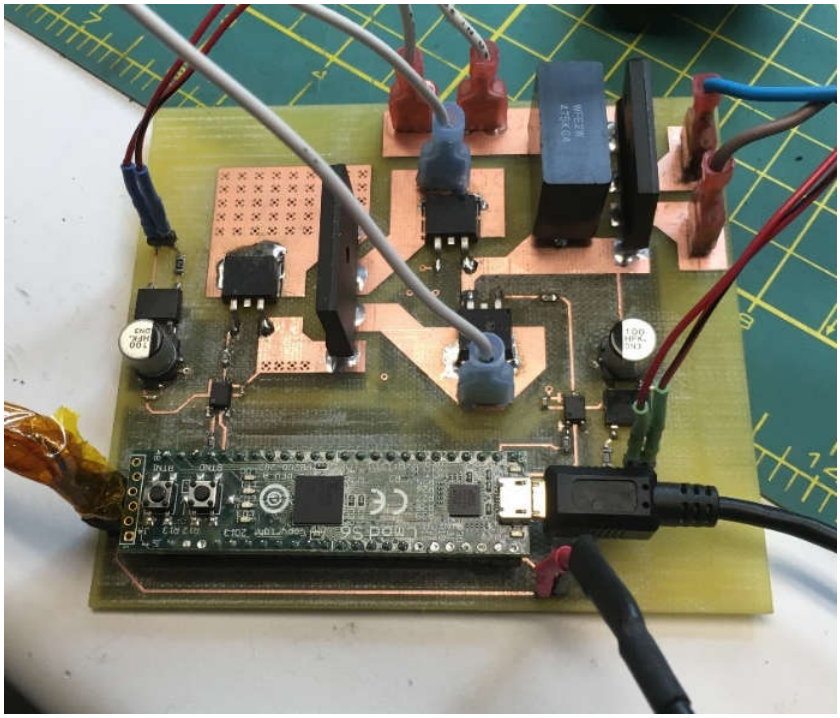

**Figure 31:** Revised Gen 4.2 prototype drive for the 1/2HP motor

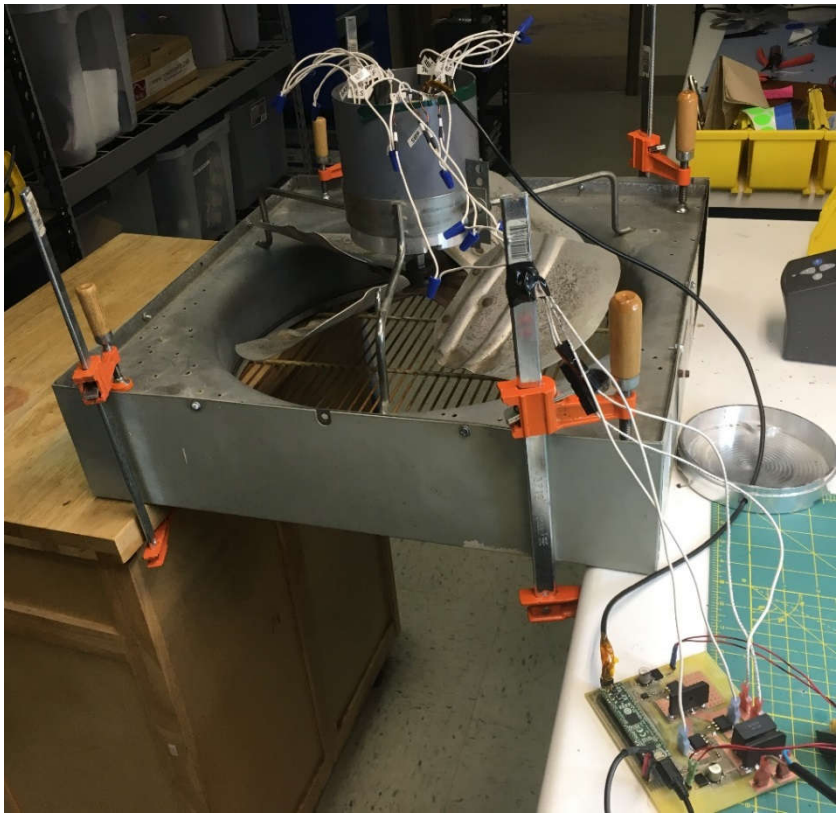

**Figure 32:** Revised Q-Sync 4.2 drive tuning and evaluation using a ½ HP motor and condenser fan assembly

Ultimately, this concept could be extended by using other combinations of stator teeth and rotor poles to create a motor with more than just two efficient, fixed speed operating points. Figure 33 shows a breadboard circuit for demonstrating 2-speed operation with the 50W motor. The breadboard circuit has been connected to the 50W motor and fan assembly for evaluation as shown in Figure 34. This demonstration circuit for 2-speed operation in a 50W motor uses a somewhat larger number of components than previous drive approaches. This prompted work to develop a simplified circuit and stator winding configuration while maintaining the functional advantages, and so a revision to the ½ HP prototype motor drive design to operate with multi-speed controls was made.

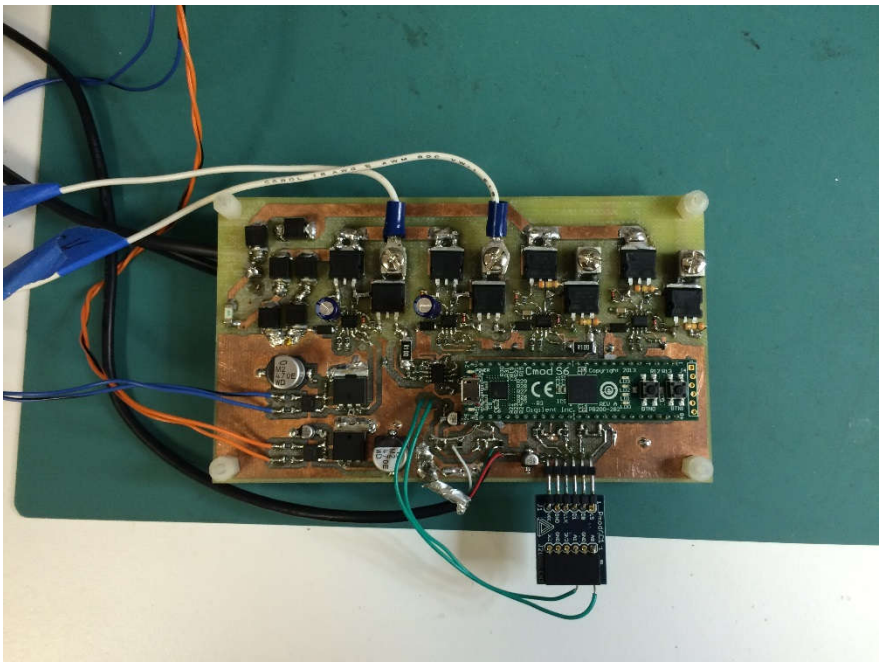

**Figure 33:** Breadboard "Multi-Speed" circuit for 50W motor demonstration

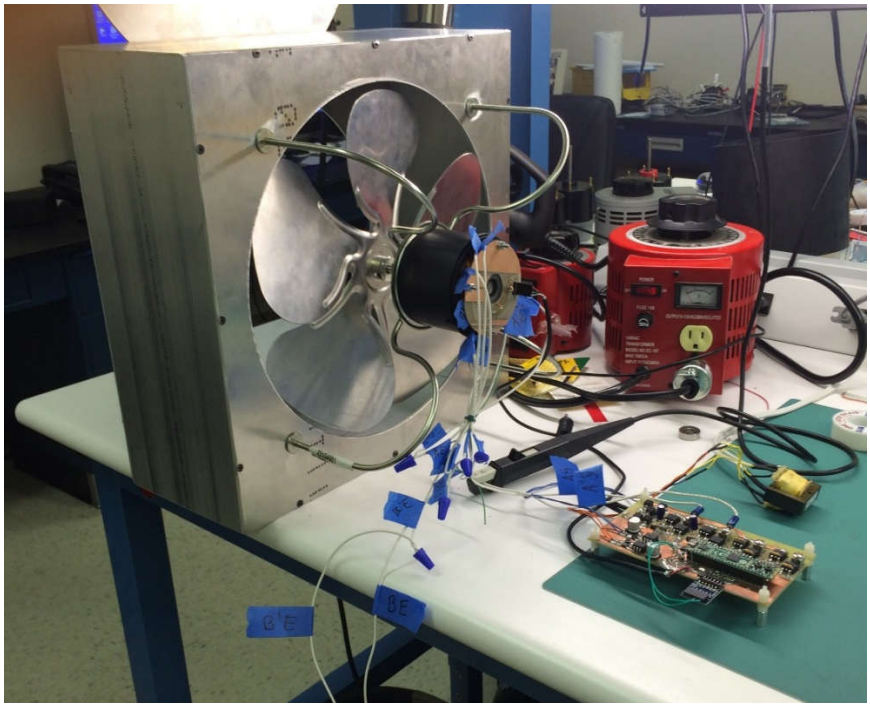

**Figure 34:** Multi-Speed demonstration set up with 50W motor and fan

Preliminary qualitative results showed good control, greatly improved torque capability, and dyno testing verified full output power capability. However, after considerable tuning and

tweaking, the energy transfer was not effective enough to prevent some power loss due to negative torque generation during transfer and so our best demonstrated efficiency with this approach was just 82%, well below the program goal of 87%. We abandoned this approach since it did not have sufficient advantage over the baseline competition.

We also continued development of the multi-speed controls. The original concept, having full speed be line synchronous (60 Hz) and lower speeds be a fraction of synchronous, is proving challenging due to large harmonic currents. We continued to investigate ways to control those currents, however, we also pursued a new variation where the line synchronous speed is the low speed of operation and full speed is a multiple of the line synchronous speed. This showed promising results in a 50W motor demonstration and we generated a revised ½ HP prototype motor design which had a synchronous speed of 600 rpm (12 pole design) for low power and will operate at twice synchronous speed for full power. We built a rotor and stator set to this design for full scale evaluation (see Figures 35 & 36).

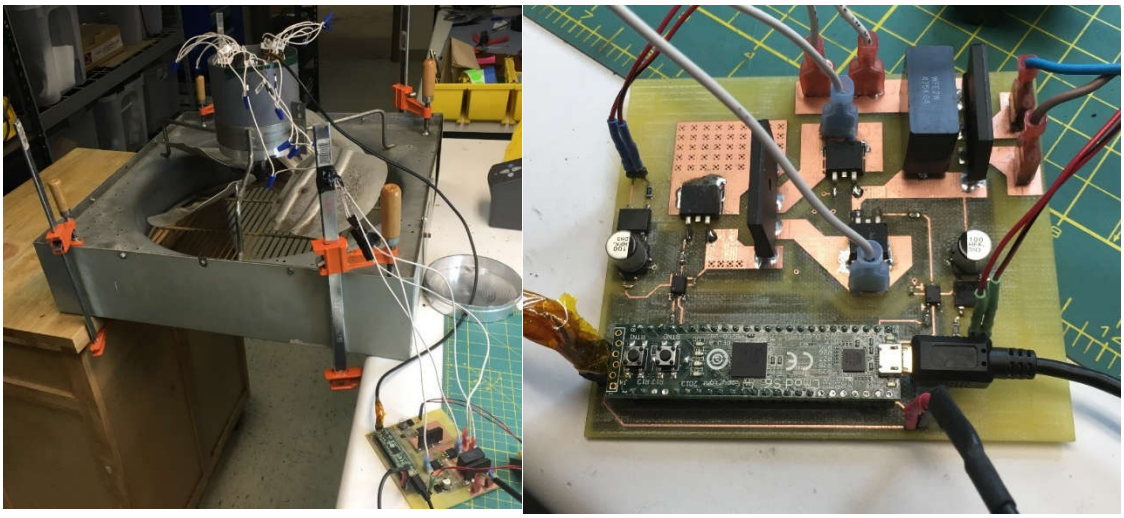

**Figure 35:** Revised Gen 4.2 prototype drive for the 1/2HP motor

With the previous arrangement (i.e., full speed synchronous), when operating at fractions of synchronous speed the back EMF is at a lower frequency than the supply voltage. We determined during our evaluation of a couple of different rotor magnet configurations for the 50W motor that the efficiency and stability of this approach are very sensitive to the shape of the back EMF waveform resulting in increased losses due to harmonic currents. We determined that having the low speed be the line synchronous speed and have the higher speed be a multiple of it was worth investigating further. While this arrangement is also somewhat sensitive to back EMF waveform, it is easier to control and had shown promising results in the 50W motor.

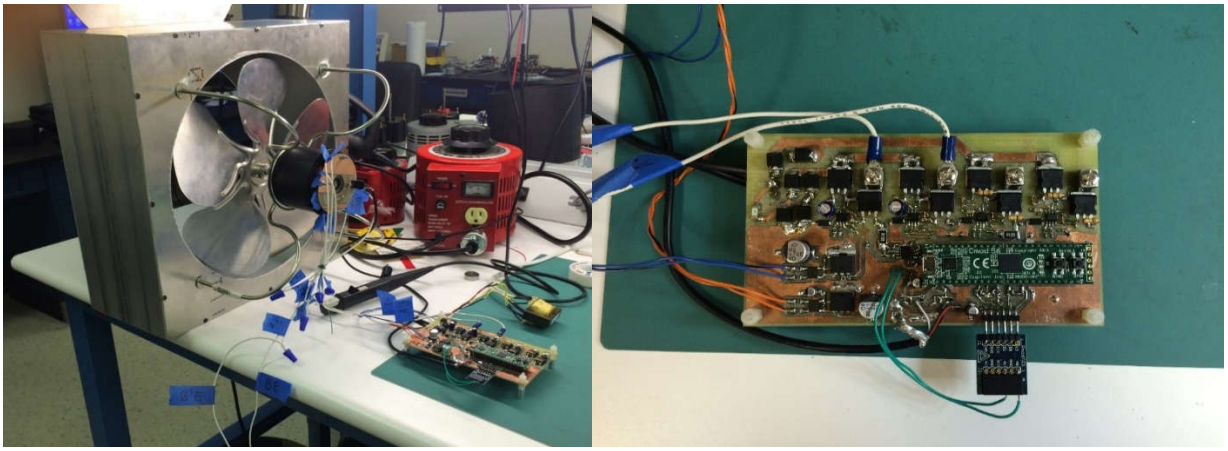

**Figure 36:** 50W "Multi-Speed" demonstration

Based on the 50W motor results we decided to revise the ½ HP prototype design for operation with this synchronous low speed, control configuration. We chose a 12 pole motor design to give a synchronous speed of 600 rpm. The full power speed of 1200 rpm was twice line synchronous speed. The revised rotor and stator are designed to fit in the existing prototype mechanical package. For expediency, the first rotor was built with more readily available neodymium iron boron magnets, with subsequent design iterations to use lower cost ceramic magnets. Figure 37 shows a finite element analysis flux density plot for one twelfth of the motor.

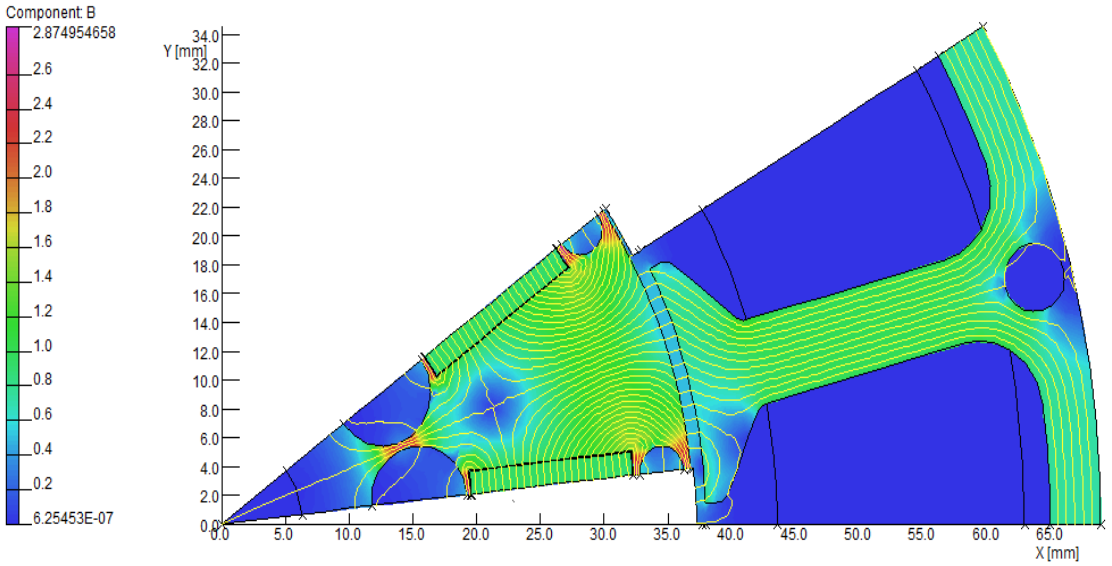


**Figure 37:** Flux density plot for revised, 12-pole, prototype design for multi-speed controls

To evaluate the performance of using low speed as the synchronous speed and twice the synchronous speed as the second speed (600 & 1200 rpm), a 12-pole 1/2HP prototype motor was built (see Figures 38 & 39); like our initial 6-pole prototype, that IPM rotor utilizes off the shelf neodymium magnets. A more cost effective design using ferrite magnets would be developed once we have demonstrated the finalized control approach. Simultaneously, efforts also continued on refining the initial controls with synchronous speed being 1200 rpm and off speed being half that with the 6-pole prototype. Further improvements to the switching algorithms for this latter (original) approach showed much better control of harmonic currents at fractional speed operation, the primary concern that led to the investigation of the alternative multiple of synchronous speed controls.

Ultimately, we found through testing that the second approach had somewhat higher losses. Figure 40 shows efficiency versus output power for the refined original two-speed approach (1200 rpm synchronous speed and 600 rpm off speed) at various supply voltages as measured on the dynamometer. As can be seen in Figure 40, peak efficiency at 1200 rpm synchronous speed reached 89%, exceeding the program goal of 87%, with .88 power factor. Having the basic control solution determined, we then set about optimizing the motor design to shift the region of peak efficiency out to higher power output levels at nominal supply voltage. Further optimization of the magnetics design was also deemed necessary to mitigate some marginal stability issues identified at fractional speeds. The recent refinements suggest the potential for better control of harmonics at ½ and 2/3 of synchronous speed compared to using a multiple of synchronous speed, which will eventually be critical as additional speeds are added to future product offerings.

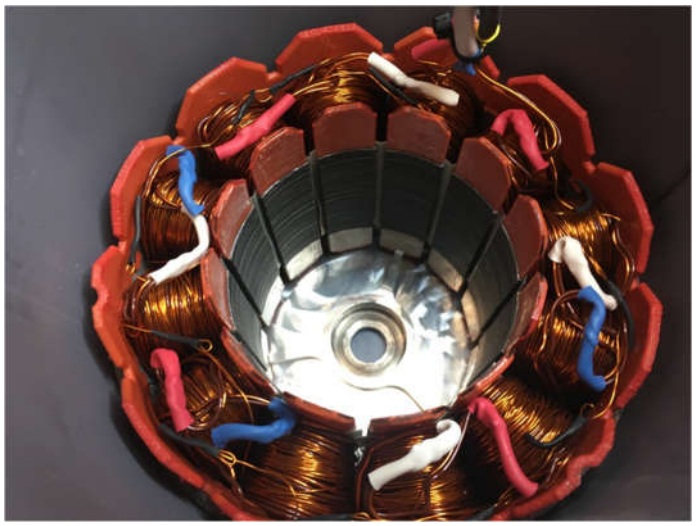

**Figure 38:** 12-pole prototype stator

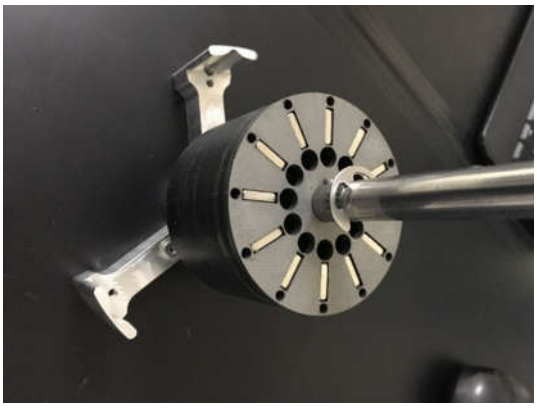

**Figure 39:** 12-pole prototype rotor, Neo version

After evaluating the two prototypes we have decided on the Type A approach with the 6-pole motor.

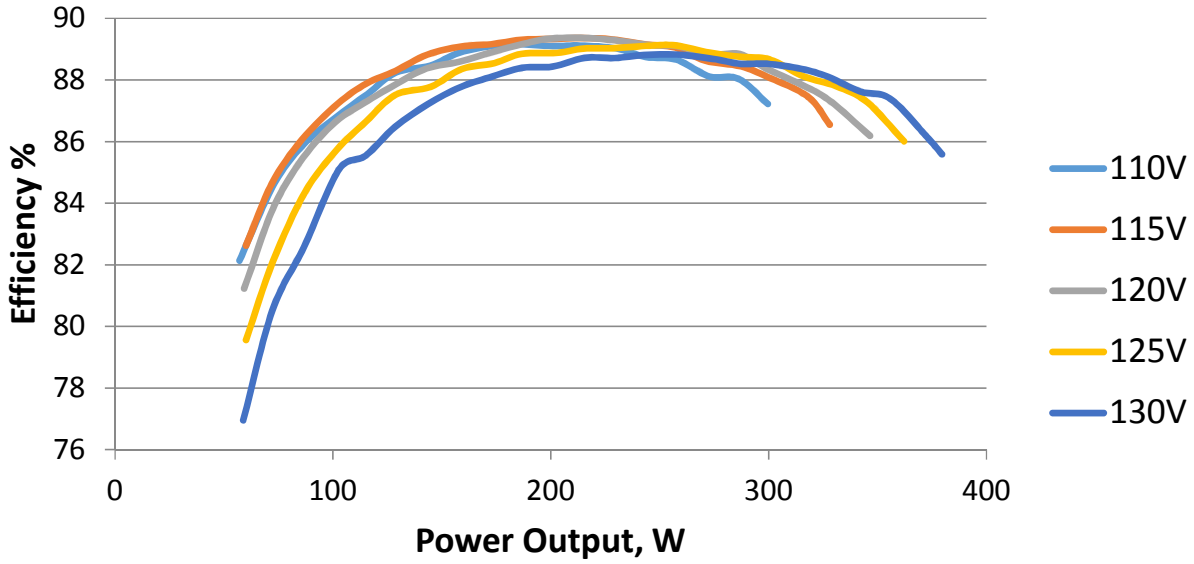


**Figure 40:** Efficiency vs. output power for the 6-pole prototype with refined "Type A" controls; further optimization was subsequently undertaken to better match peak efficiency and rated power output at nominal voltage

Having settled on a control approach meeting our peak efficiency goal, we then went about optimizing the magnetics design for best overall performance and improved stability, integrating the electronics with the motor housing, and considering cost-performance trade-offs, leading to a full final prototype evaluation. An additional prototype for the Type A controls approach (i.e., full synchronous speed and 1/2 synchronous speed) was fabricated with

a six pole full load line synchronous motor with ferrite instead of rare-earth magnets (the latter of which would be cost-prohibitive in production models). To build this prototype, we removed surface mount ferrite magnets from a competitor's motor, cut the magnets down to a different size, re-magnetized them, and assembled them onto our rotor. Doing this allowed us to shape the back EMF waveform into a more sinusoidal wave shape, while also lowering the inductance/impedance of the motor coils. Using this design configuration, we were able to shift the peak efficiency out closer to a ½ HP load, while still maintaining 89% peak efficiency, and increase the power factor from .88 to .95.

Drive Fabrication, Tuning, and Testing

After deciding to move forward with the Type A controls, wherein rated speed is line synchronous, we made a new six-pole stator with a ferrite rotor. The stator and rotor assemblies for this prototype are shown in Figures 1 and 2. Unlike the previous designs that used off the shelf neodymium magnets, in part because they are more readily available in standardized prototype sizes, this design shows that more cost effective ferrite magnets can achieve similar performance results to the neodymium magnets. This stator was wound only for full speed to allow us to fully refine full speed operation on the Type A controls, including making changes to the windings without having to remove the second speed winding. Notably, the decision to revert to surface mounted magnets on the rotor instead of an IPM rotor design was made because the IPM device was found to have too much reluctance, thus preventing us from reaching full load. The new stator and rotor for this prototype can be seen in figures 41 & 42.

**Figure 41:** 6-pole prototype stator

**Figure 42:** 6-pole surface mounted prototype rotor, with ferrite magnets

The efficiency improvement realized in the last prototype from using the switching algorithms for this selected controller approach were maintained with the further refined controller circuit employed. Figure 43 shows efficiency vs. output power for various supply voltages as measured on the dynamometer. Peak efficiency reaches 89%, in excess of our program goal of 87%. Despite this improvement, it was decided to continue to refine the design to move the efficiency curve further to the right to better align efficiency points with the full 1/2 HP rated power targeted.

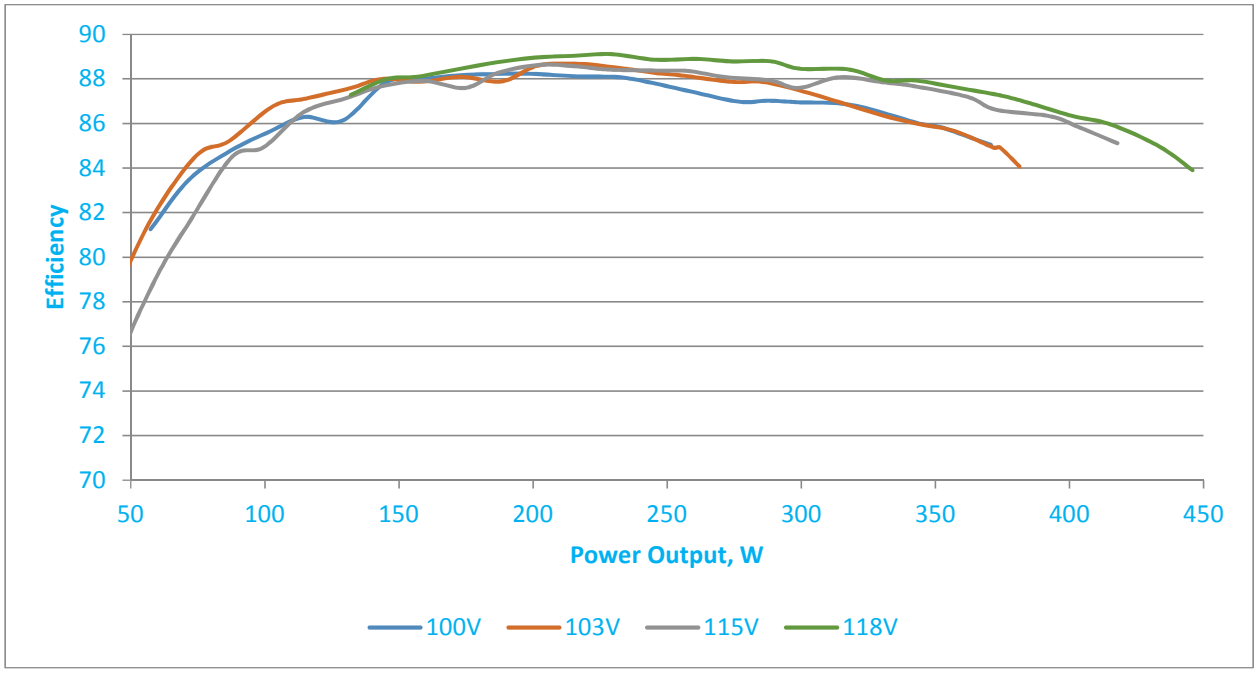


**Figure 43:** Efficiency vs. output power for the 6-pole prototype with refined Type A controls; more optimization work was subsequently done to better match peak efficiency and power point at nominal voltage

As previously reported, the use of ferrite magnets is necessary to achieve cost targets. While our initial ferrite magnet prototype's performance met project goals, additional work was performed to address stability and demagnetization issues encountered. This work resulted in us being better able to shape the back EMF waveform into a more sinusoidal wave shape, while also lowering the inductance/impedance of the motor coils. This was accomplished by reshaping and re-magnetizing ferrite magnets we used in the previous prototype. This new ferrite prototype demonstrated improved performance. It was hoped that a new prototype using newly custom-ordered magnets would be built and tested during the reporting period, however, supply chain difficulties and the project end date precluded that possibility.

In conclusion, a final fully-functional prototype using custom ordered magnets and employing two speeds was not built, but the overall project goals were realized through previously built prototypes. More specifically, a multi-speed 1/2 HP fan motor with greater than 87% peak efficiency and greater than 0.9 power factor at full speed, with comparable performance to existing ECM levels at a second speed in the same NEMA 48-frame sized HVAC fan motor was designed, fabricated and tested. Tests of the two-speed prototype confirm the technical viability of QM Power's innovative designs, and further tests of ferrite versions show that the same superior efficiency and power factor levels are indeed possible utilizing the more economical ferrite magnets. Though the initial ferrite magnet prototype was not wound for multi-speed operation, the fact that it uses the same control mechanisms for two speed operation, and that they are the same regardless of which type of magnets are used, suggest that the second "off" speed performance should still be comparable to ECM peak performance with ferrite magnets (~80% efficiency and 0.7 power factor). The initial ferrite magnet prototype's full load efficiency was 89%, with >0.9 power factor. Though a version with customized magnets was not fabricated, a second ferrite prototype using magnets from the initial prototype that were modified and re-magnetized, and incorporating a longer rotor and modest software changes was built and tested during the reporting period and found to have 90% efficiency without sacrificing power factor. Figure 44 shows a picture of the second ferrite motor prototype. Figure 45 shows the efficiency curves at various voltages for the second ferrite prototype. Figure 46 shows the motor's efficiency and power factor curves on a single chart at 115 volts. Finally, Figures 47 & 48 show airflow tests on the final prototype with various blades operating at 1200 rpm compared to an ECM that is representative of the baseline motor. Figure 47 shows airflow versus static pressure and versus power consumption. Figure 48 shows airflow versus static pressure and versus current draw. The charts, which have red shaded lines for the QMP motor and blue shaded lines for the ECM show the clear superiority of the new QMP prototype, which consistently uses less power for the same airflow; the current draw was also substantially reduced with the QMP solution, including in cases where the Q-Sync motor is moving considerably more cfm, owing to the much higher power factor at full speed.

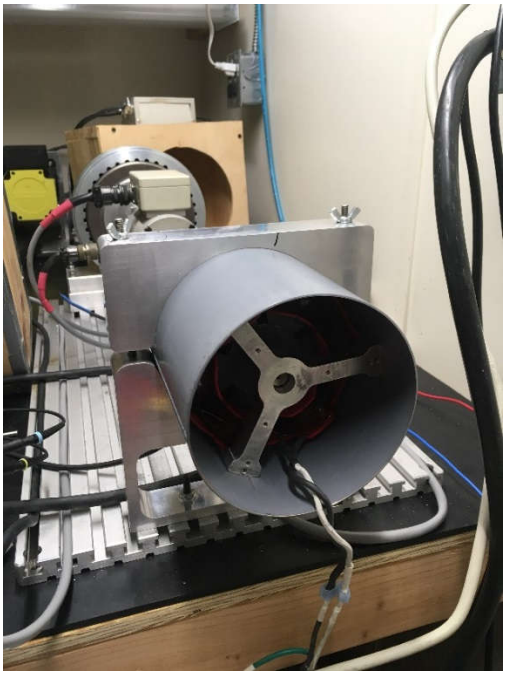

**Figure 44:** The second 6-Pole 1/2 HP motor with the longer rotor on the test bed

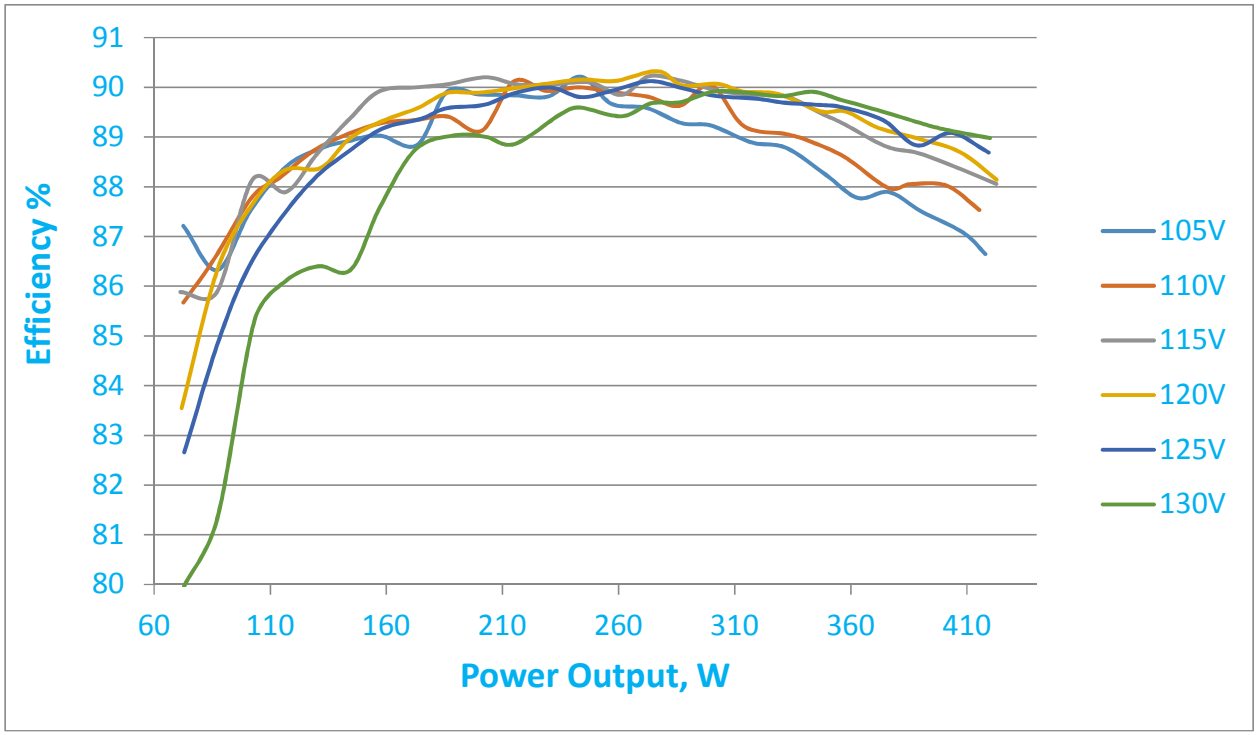


**Figure 45:** Efficiency vs. output power for the 6-pole prototype with refined Type A controls, re-worked and re-magnetized ferrite magnets and a longer rotor

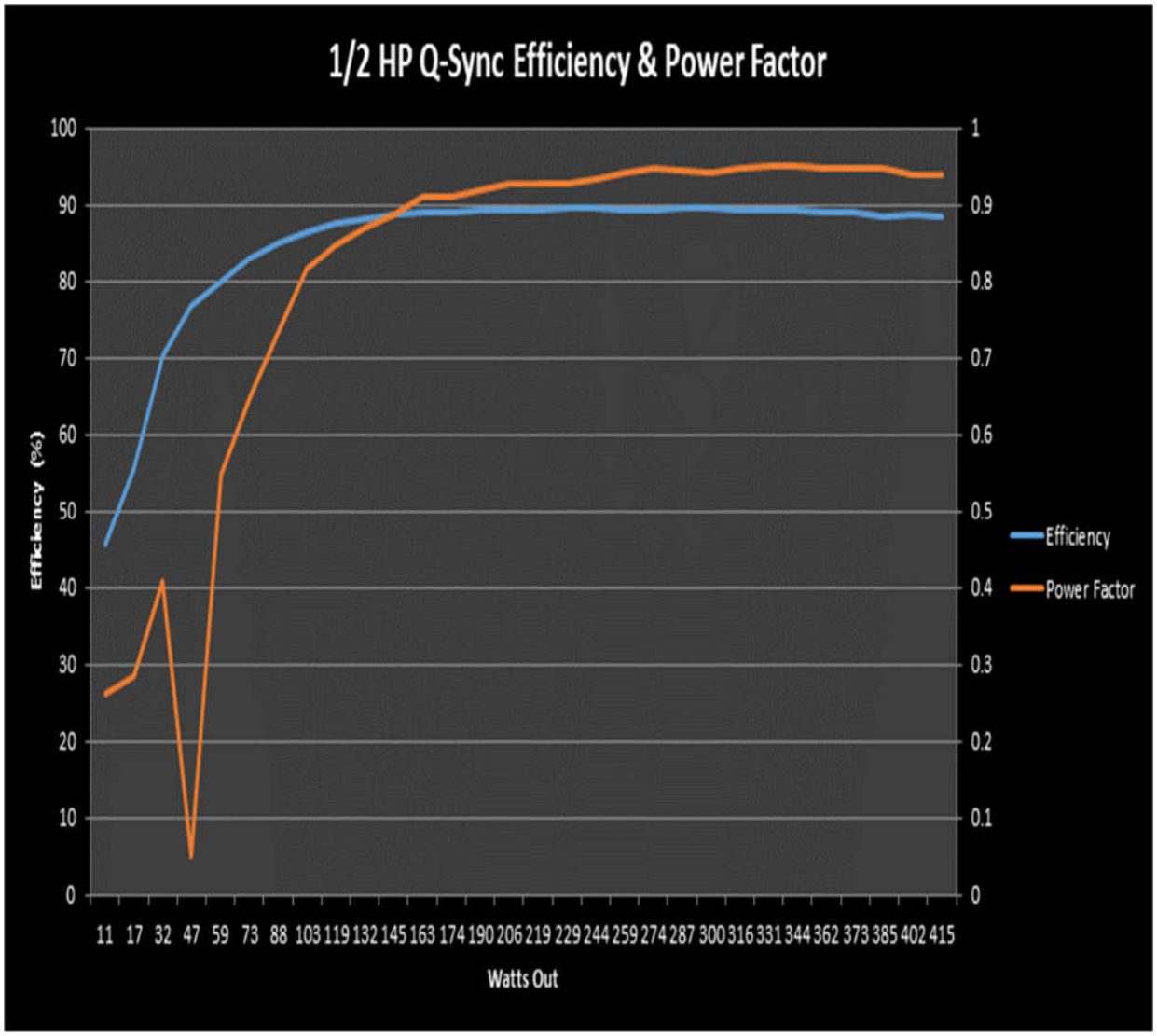


**Figure 46:** Efficiency & power factor curves for the final prototype at 115 volts

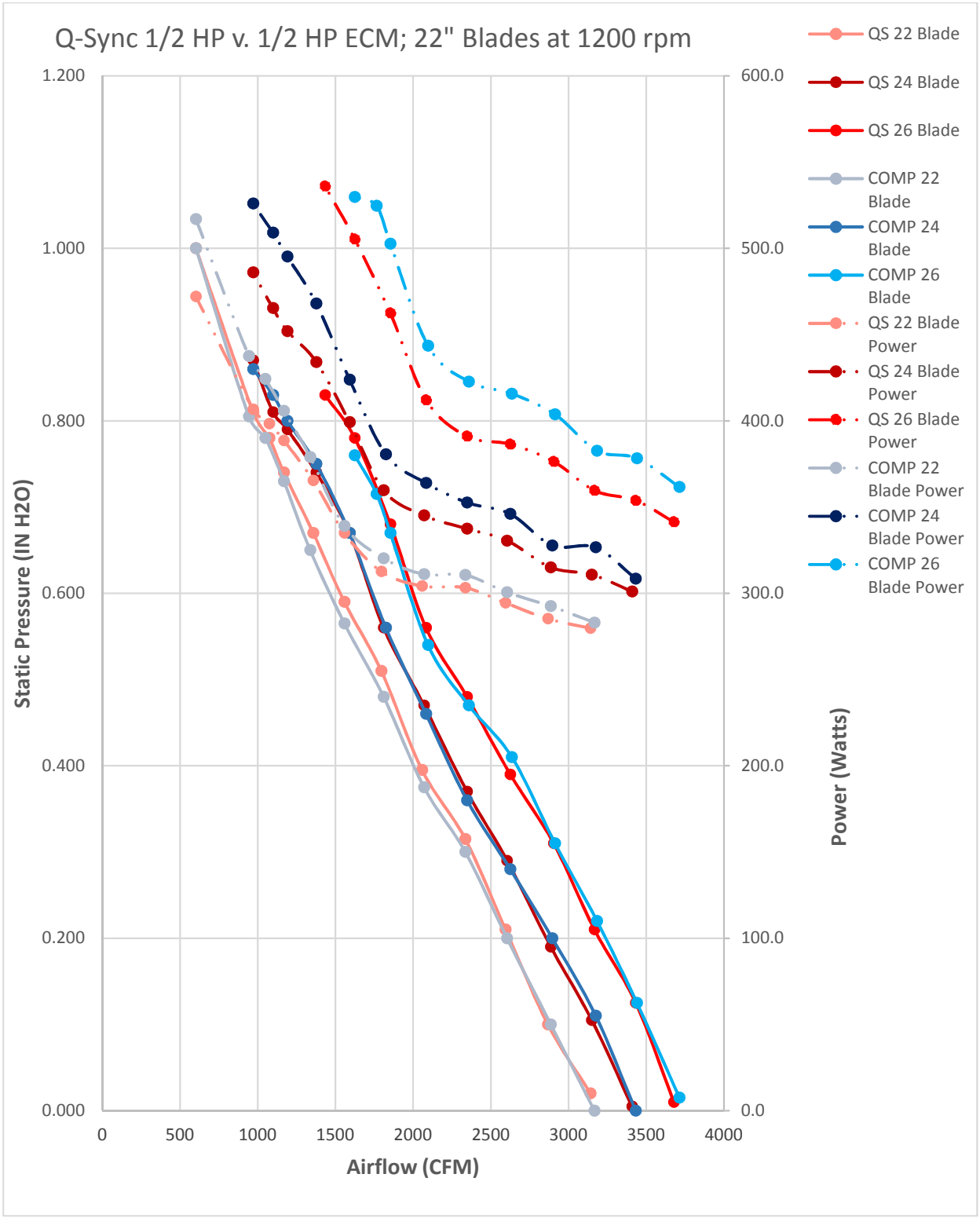


**Figure 47:** Airflow curves with cfm versus static pressure (left Y-axis and solid lines) and power consumption (right Y-axis and dashed lines); Q-Sync in red shades, ECM in blue shades

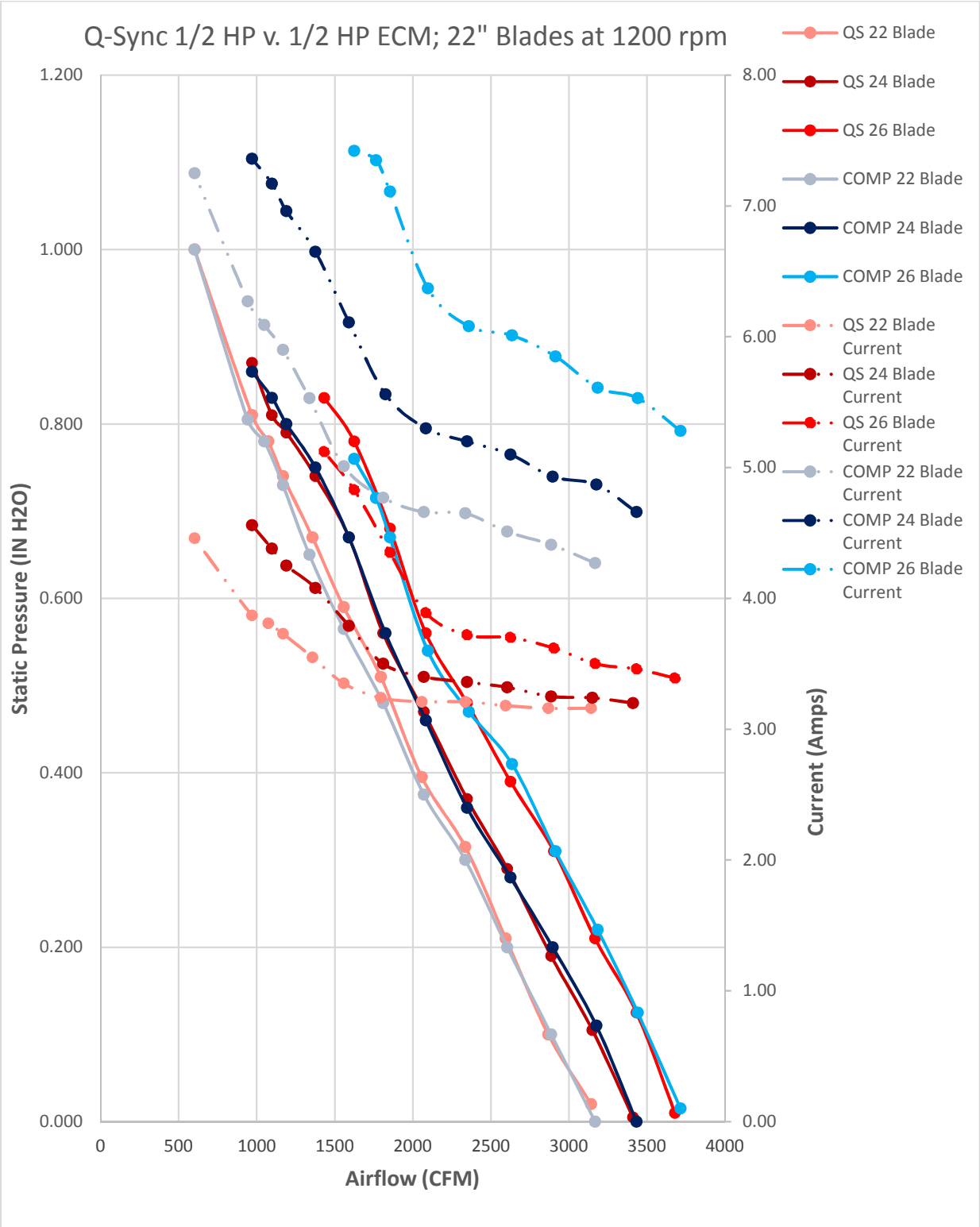


**Figure 48:** Airflow curves with cfm versus static pressure (left Y-axis and solid lines) and current draw (right Y-axis and dashed lines); Q-Sync in red shades, ECM in blue shades